THESIS FOR THE DEGREE OF DOCTOR OF PHILOSOPHY

PROBING SECRETORY VESICLES AND LIPOSOME MODEL SYSTEMS USING NANOSCALE ELECTROCHEMISTRY AND MASS SPECTROMETRY

JELENA LOVRIĆ

Department of Chemistry and Chemical Engineering

CHALMERS UNIVERSITY OF TECHNOLOGY

Gothenburg, Sweden 2016

Probing secretory vesicles and liposome model systems using nanoscale electrochemistry and mass spectrometry

Jelena Lovrić

ISBN: 978-91-7597-415-6

Doktorsavhandlingar vid Chalmers tekniska högskola
Ny serie nr 4096
ISSN 0346-718X

Department of Chemistry and Chemical Engineering
Division of Chemistry and Biochemistry
Analytical Chemistry
Chalmers University of Technology
SE-412 96 Gothenburg
Sweden
Telephone: +46 (0)31 772 1000

Front cover: The transmitter content of the vesicles is analyzed by secondary ion mass spectrometry imaging. By acquiring mass spectrum for each pixel, chemical maps can be obtained (top). Vesicle electrochemical cytometry can be employed to analyze electroactive content of single vesicles. The spike in the amperometric trace provides quantitative data by employing Faraday's law. The integration of the area below the spike gives the charge (Q) that is directly proportional to the amount of vesicle electroactive content (bottom).

Back cover: Photo of the author © Mats Tiborn

Printed by Chalmers Reproservice
Gothenburg, Sweden 2016

Probing secretory vesicles and liposome model systems using nanoscale electrochemistry and mass spectrometry

JELENA LOVRIĆ

Department of Chemistry and Chemical Engineering
Chalmers University of Technology

Abstract

Cellular communication is based on the process of exocytosis, regulated release of chemical messengers into the extracellular space. These messengers, neurotransmitters, are packed into vesicles that during exocytosis fuse with the plasma membrane and release their content. Much work has been done to understand the mechanism of exocytosis, whether it is full or transitory transmitter release or a combination of these modes of exocytosis. However, its full comprehension is still under debate. One of the important pieces of the exocytosis puzzle and relevant evidence for the fractional exocytosis, is probing the entire neurotransmitter content of secretory vesicles. Despite the challenge to achieve this, owing to small vesicle size and often less than an attomole of detectable material, advances in bioanalytical techniques have allowed measurements at higher spatial resolution and with decreasing amounts of analytes. In this thesis, I have employed electrochemical techniques and imaging mass spectrometry as analytical tools to study the content of large dense core vesicles of neuroendocrine cells and liposome systems as secretory vesicle models.

In the first part of the thesis work, Papers I and II, I applied a new amperometric technique called vesicle electrochemical cytometry to measure the catecholamine content in native vesicles and liposomes. In Paper I, this technique was employed to quantify the content of catecholamines present in single mammalian vesicles isolated from cells of the bovine adrenal gland. Paper II represents the continuation of work done in Paper I, where the same experimental setup was employed with focus on investigation of the mechanism of vesicle rupture onto the electrode by applying a bottom up approach and probing the transmitter loaded liposomes. The second part of this thesis, Papers III, IV and V, describe the application of imaging mass spectrometry to reveal the chemical composition of vesicles and liposomes. In Paper III, time-of-flight secondary ion mass spectrometry (ToF-SIMS) was employed to study the chemistry of micrometer size liposome models containing histamine and liposomes containing an aqueous two-phase system, both to mimic secretory vesicles. Paper IV demonstrates the potential of ToF-SIMS to evaluate the preservation capabilities of chemical fixation, a common approach for sample preparation in subcellular imaging as well as a screening tool for optimization of high-resolution NanoSIMS imaging. In Paper V, NanoSIMS, and electrochemical techniques were used in combination, to study the neurochemistry of large dense core vesicles from PC12 cells. The major goals were to investigate the impact of pharmaceuticals like L-3,4-dihydroxyphenylalanine and reserpine on metabolic pathways of neurotransmitter dopamine and to quantify dopamine content in PC12 vesicles, one vesicle at a time and in subvesicular regions.

Keywords: *Exocytosis, neuroendocrine cells, large dense core vesicles, liposomes, neurotransmitters, electrochemistry, vesicle electrochemical cytometry, amperometry, ToF-SIMS, NanoSIMS.*

List of publications

The thesis is based on the work contained in the following papers, referred by Roman numerals in the text:

I. **Characterizing the catecholamine content of single mammalian vesicles by collision–adsorption events at an electrode**
Johan Dunevall, Hoda Fathali, Neda Najafinobar, Jelena Lovrić, Joakim Wigström, Ann-Sofie Cans, & Andrew G. Ewing
J. Am. Chem. Soc., 2015, 137 (13), pp 4344–4346, DOI: 10.1021/ja512972f

II. **On the mechanism of electrochemical vesicle cytometry: chromaffin cell vesicles and liposomes**
Jelena Lovrić,[§] Neda Najafinobar,[§] Johan Dunevall, Soodabeh Majdi, Irina Svir, Alexander Oleinick, Christian Amatore, & Andrew G. Ewing
Faraday Discuss., 2016, DOI: 10.1039/C6FD00102E

III. **Analysis of liposome model systems by time-of-flight secondary ion mass spectrometry**
Jelena Lovrić, Jacqueline D. Keighron, Tina B. Angerer, Xianchan Li, Per Malmberg, John S. Fletcher, & Andrew G. Ewing
Surf. Interface Anal., 2014, 46, 74–78, DOI: 10.1002/sia.5623

IV. **Multimodal imaging of chemically fixed cells in preparation for NanoSIMS**
Jelena Lovrić, Per Malmberg, Bengt R. Johansson, John S. Fletcher, & Andrew G. Ewing
Anal. Chem., 2016, Article ASAP, DOI: 10.1021/acs.analchem.6b02408

V. **Dopamine storage, one vesicle at a time**
Jelena Lovrić, Johan Dunevall, Anna Larsson, Lin Ren, Shalini Andersson, Anders Meibom, Per Malmberg, Michael E. Kurczy, & Andrew G. Ewing
Manuscript

[§] These authors contributed equally to the work

Related publications not included in the thesis

Extracellular osmotic stress reduces the size and adjusts the catecholamine content of secretory vesicles to maintain a constant catecholamine concentration
Hoda Fathali, Johan Dunevall, Soodabeh Majdi, Jelena Lovrić, Andrew G. Ewing, & Ann-Sofie Cans
Submitted

Excited fluorophores enhance the opening of vesicles at electrode surfaces in vesicle electrochemical cytometry
Neda Najafinobar, Jelena Lovrić, Soodabeh Majdi, Johan Dunevall, Ann-Sofie Cans, & Andrew Ewing
Submitted

Lithographic microfabrication of a 16-electrode array on a probe tip for high spatial resolution electrochemical localization of exocytosis
Joakim Wigström, Johan Dunevall, Neda Najafinobar, Jelena Lovrić, Jun Wang, Andrew G. Ewing, & Ann-Sofie Cans
Anal. Chem., 2016, 88 (4), pp 2080–2087, DOI: 10.1021/acs.analchem.5b03316

Combined isotopic and optical nanoscopy
Katharina N. Richter,[§] Silvio O. Rizzoli, & Jelena Lovrić[§]
Submitted

Quantitative chemical measurements of vesicular transmitters with single cell amperometry and electrochemical cytometry
Jelena Lovrić, Xianchan Li, & Andrew G. Ewing, Chapter 8, in "Compendium of In-Vivo Monitoring in Real-Time Molecular Neuroscience: Volume 1: Fundamentals and Applications", World Scientific Publishing Company, Singapore, 2014.
Book chapter

[§] These authors contributed equally to the work

Contribution report

Paper I: I contributed in designing and performing the experiments with J.D. Contributed in editing the paper.

Paper II: I was involved in designing the experiments. Performed experiments and analyzed the data with N.N. I outlined the manuscript with authors. I contributed in writing the first draft of the manuscript as well as edited with other authors.

Paper III: Designed the experiments with J.D.K, P.M and J.S.F. Performed the experiments and analyzed the data together with P.M, J.S.F and T.B.A. I outlined the manuscript with authors and wrote the first draft of the manuscript as well as edited with other authors.

Paper IV: I was involved in designing the experiments. Performed experiments together with P.M. I analyzed the data. I outlined the manuscript with authors and wrote the first draft of the manuscript as well as edited with other authors.

Paper V: I designed the NanoSIMS experiments and discussed with others the protocols for the electrochemistry experiments. I conducted the TEM and NanoSIMS imaging and wrote the first draft of the manuscript. All authors discussed the results, outlined and commented on the manuscript.

Contents

List of abbreviations

AADC	Aromatic amino acid decarboxylase
ATPS	Aqueous two-phase system
CCD	Charge-coupled device
Cg	Chromogranin
DOPC	1,2-dioleoyl-sn-glycero-3-phosphocholine
DOPE	1,2-dioleoyl-sn-glycero-3-phosphoethanolamine
GUV	Giant unilamellar vesicle
IMS	Imaging mass spectrometry
L-DOPA	L-3,4-dihydroxyphenylalanine
LDCV	Large dense core vesicle
LMIG	Liquid metal ion gun
LUV	Large unilamellar vesicle
NTA	Nanoparticle tracking analysis
PC12	Pheochromocytoma cell line
PEG	Polyethylene glycol
PNMT	Phenylethanolamine-N-methyl transferase
PNT	Plasma membrane neurotransmitter transporter
SCA	Single cell amperometry
SEM	Scanning electron microscopy
SIMS	Secondary ion mass spectrometry
STR8	Stearyl-octaarginine
SUV	Small unilamellar vesicle
TEM	Transmission electron microscopy
ToF-SIMS	Time-of-flight secondary ion mass spectrometry
VEC	Vesicle electrochemical cytometry
VMAT	Vesicular monoamine transporter
VNT	Vesicular neurotransmitter transporter

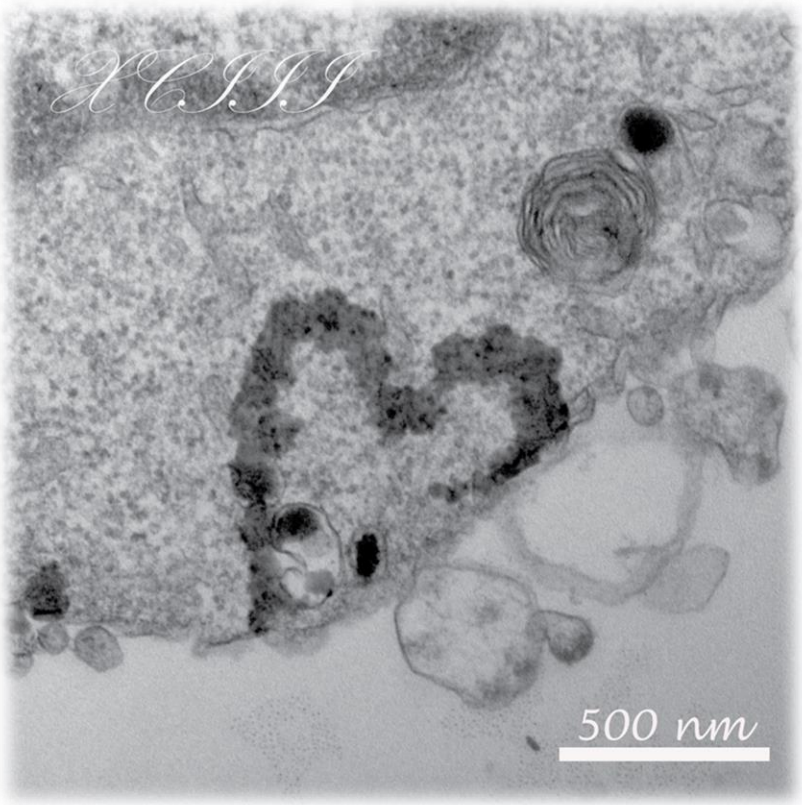

Love is for All

A transmission electron microscopy image of a neuroendocrine cell (PC12) showing the heavy metal heart encapsulating a loving couple of neurotransmitter secretory vesicles. © Jelena Lovrić, March 15, 2016

1 CELLULAR COMMUNICATION

Like people and complex multicellular organisms, individual cells have a need to sense the environment and respond to the surrounding stimuli. Thus, a typical living cell in order to function harmoniously with the Universe, must be able to sniff, sense, detect and avoid the elements and components present in the neighboring environment. Simply, it must have the ability to communicate with other cells. In basic terms, cell signaling is comprised of two parties, the signaling cell that initiates the message and the target cell that receives the signaling message and converts it to the intracellular signal that directs the cell behavior. Often the signal that is passing between the cells, even though it represents the same information, has to change form in order to propagate across the long distances and reach the receiving cell. Therefore, it has to be transduced.

The broadcasting of the signal can be categorized as four different types. Hence, the signal can be transmitted from the endocrine cells *through the bloodstream* via hormone molecules. The less 'public' way is *paracrine signaling*, such as regulation of inflammation, via local mediators that diffuse across the extracellular space and remain nearby the excreting cell. There is also an 'intimate' communication, a *short range signaling* between the cells that do not have a need to secrete the messenger molecules, but communicate through the contact between their plasma membranes. Lastly, neurons are characterized by a *neuronal signaling* that is comprised of electrical and chemical signal broadcasting. The electric signal is transmitted over long distances very quickly via an action potential, but through the neuronal cell itself via the cell axon. When the electric stimulus reaches the axonal terminal, in order to be able to be received by the neighboring neuron, it must pass over a <100 nm gap, called the synapse. However, as the electric signal cannot cross over the non-conductive moiety present in the synapse, it is transduced into a chemical message, and the molecule that carries the signal is called the *neurotransmitter*. Hence, an each electric impulse initiates the axon terminal of the *presynaptic cell* (signaling cell) to secret a quanta of chemical messengers that is expelled into the synaptic gap and received by the neighboring neuron, called the *postsynaptic cell* (receiving cell). The essential and rather complicated process by which the transmitters are released, and consisting of several phases, is called *exocytosis*.[1,2]

1.1. Exocytosis

In endocrine cells and neurons, chemical signaling relies on neurotransmitters release. This is mediated by the exocytosis of nanometer size organelles called secretory vesicles. In neurons, synaptic transmission is triggered at the presynaptic nerve terminal with an action potential that induces the opening of voltage-gated calcium channels.[3] The influx of Ca^{2+} ions into the cytoplasm stimulates vesicle exocytosis at the presynaptic active zone and the vesicle trafficking cycle begins.[1,4,5]

Vesicle trafficking is composed of several steps (Fig. 1). Vesicles are loaded with neurotransmitters by active transport via the vesicular neurotransmitter transporter (VNT). They cluster together in a reserve pool inside the cell and near the presynaptic terminal. In the following steps, the vesicles dock to the plasma membrane and in an ATP-dependent manner, a priming phase occurs that makes the vesicles ready to respond to the formation of a Ca^{2+}-triggered fusion pore initiating release. Docking, priming and fusion of the vesicles with the plasma membrane generally recruit three SNARE proteins, synaptobrevin, a vesicle membrane protein, and two plasma membrane proteins, syntaxin-1 and SNAP-25. Even though there is a general agreement that the SNARE proteins are involved in the fusion event, their detailed activity is still under debate. It was proposed that the SNARE proteins form a complex that pulls the synaptic vesicle and plasma membrane close to each other into an intermediate state before fusion. After the cytoplasmic influx of calcium through the voltage-gated channels, the SNAREs draw the vesicle closer to the plasma membrane and this close contact induces formation of the fusion pore. The fusion pore is an opening that allows neurotransmitters to escape into the synaptic cleft and thereafter the vesicles can close again or undergo endocytosis and recycle for the next trafficking cycle. When vesicles are fully opened and then undergo endocytosis the recycling phase involves re-acidification of the vesicle interior and active neurotransmitter refilling via VNTs.[1,6,7] Most of the chemical messengers are cleared out from the synapse after exocytotic release. The reuptake of the transmitters across the plasma membrane is done by a plasma membrane neurotransmitter transporter (PNT). This reuptake is dependent on the cotransport of Na^+ and Cl^- ions and the vesicular neurotransmitter storage relies heavily on this reuptake.[8,9]

The destiny of the secretory vesicles after the fusion event has been much debated. If the vesicles completely collapse into the plasma membrane and release total content, the fusion event called *all-or-none* would avoid the recycling process of the valuable vesicle lipid and protein

components, necessary for the vesicle availability and thus sustained chemical signaling.[10] Therefore, much work has been done to observe the transient fusion of secretory vesicles and several mechanisms of vesicle retrieval have been suggested.[11-16]

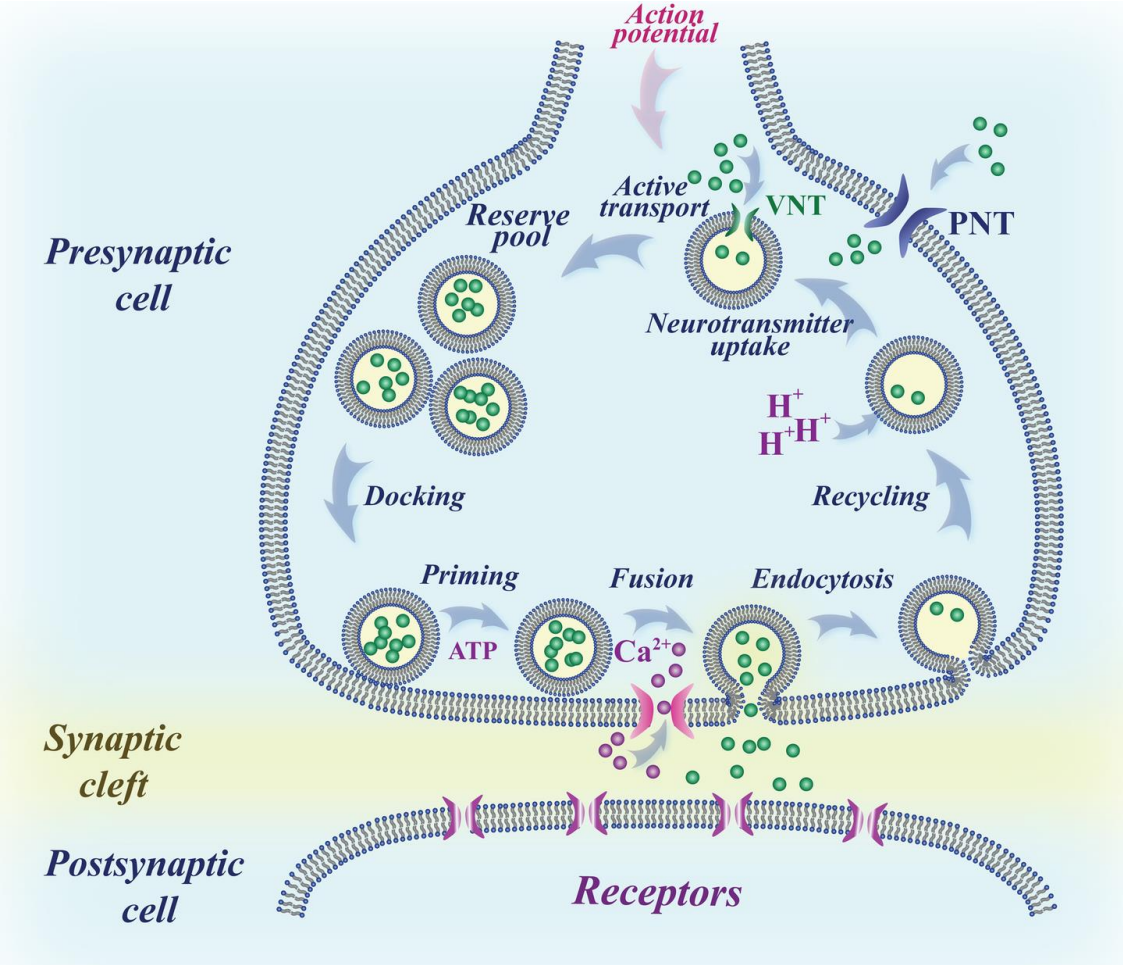

Figure 1. Schematic representation of the vesicle cycle involving exocytosis. Synaptic vesicles filled with neurotransmitter (symbolized as green spheres) dock to the plasma membrane and undergo ATP-dependent priming phase. This is followed with the fusion that is triggered by the influx of the Ca^{2+} ions. The vesicles are recycled via the endocytosis phase. Extracellular neurotransmitters are transported back into the cell via plasma membrane neurotransmitter transporter (PNT) and vesicular neurotransmitter transporter (VNT) is responsible to load the chemical messengers back into the vesicle.

The proposed modes of partial release include *flickering fusion,*[12] *kiss-and-run* exocytosis,[17,18] and *extended kiss-and-run* exocytosis.[19] After full release, vesicles are recaptured via endocytosis by clathrin-coated pits and from there, refill directly or via the endosomes. However, vesicles in kiss-and-run and extended kiss-and-run exocytosis, after the transmitter expulsion, undock and recycle locally by re-acidification and reuptake of the neurotransmitter before returning to the reserve pool and participating in the next exocytosis cycle (Fig. 1).[6]

1.2. Secretory vesicles

Chemical signaling relies heavily on the constitutive exocytosis and transient events of the neurotransmitter expulsion from secretory vesicles. In neurons two types of secretory vesicles are present, *small synaptic vesicles* (SSVs) that store and secrete classical neurotransmitters such as acetylcholine, glutamate, GABA and *large dense core vesicles* (LDCVs) which are responsible for storage and exocytotic release of monoamines, neuropeptides, and neurohormones.[5,20] Neuroendocrine cells also possess two types of transmitter vesicles, *synaptic-like microvesicles* (SLMVs) that are the counterparts of SSVs and LDCVs, often called secretory granules (Fig. 2).[21] The inner morphology, exocytosis kinetics and cytoplasmic distribution differ between small and dense core vesicles. The SSVs are clear particles with a diameter of about 50 nm, whereas LDCVs show inner morphology with a lumenal protein granule visible in electron microscopy images and have a diameter between 100-300 nm.[22] Since much work in this thesis has been done focusing on LDCVs, their principal characteristics will be covered in this section.

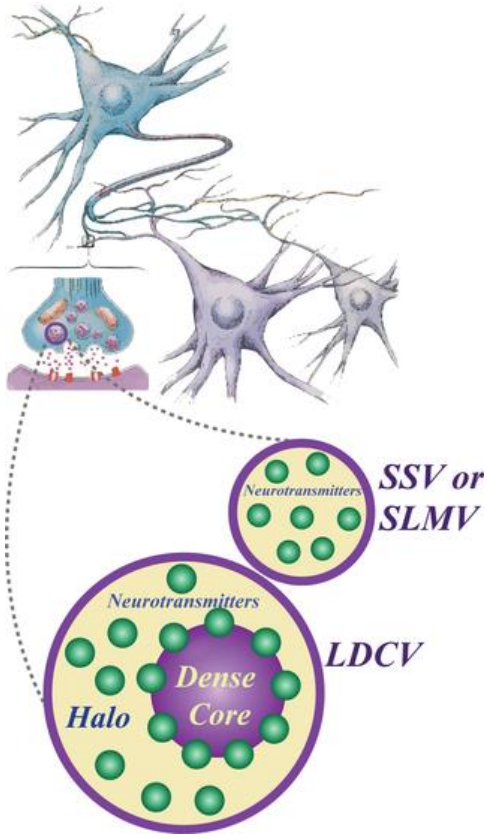

Figure 2. Types of secretory vesicles present in neurons and neuroendocrine cells. SSV – Small synaptic vesicle (in neurons); SLMV- Synaptic-like microvesicle (in neuroendocrine cells); LDCV – Large dense core vesicles (in both cell types). Neurotransmitters are symbolized as green spheres.

The biogenesis pathway of LDCVs begins with direct budding of immature secretory granules from the trans-Golgi network (TGN). Their development into mature LDCVs happens by fusing with other immature granules followed by removal of excess membrane, joining the two structures.[23] Since the protein core in LDCVs can be only synthesized in the TGN, it seems that secretory granules end their life during fusion with the plasma membrane in the exocytosis process. However, some evidence supports the idea of granule recycling back in the TGN rather than being newly synthesized.[24]

In accordance with the name of the secretory LDCVs, their primary attribute is the inner two-compartment morphology. It manifests as the electron dense *protein core* and the electron lucent

surrounding solution, called the *halo* that are observed in transmission electron microscopy images of cells in rat pheochromocytoma of adrenal medulla, (PC12) cells.[25]

Eighty percent of the total LDCV protein is found within the inner vesicular space and the main part of this protein content has been assigned to *chromogranins* (Cgs), a set of the three acidic proteins, chromogranin A, B and lesser extent chromogranin C with molecular masses of 48 k, 76 k and 67 k Da, respectively.[26,27] Chromogranin A (CgA) was the first discovered granule protein in 1969 by Helle et al. while observing the co-secretion of the water-soluble, granule-specific protein (CgA) and catecholamines by perfusing the adrenal gland.[28] Cgs proteins have several functions, such as a role in biogenesis of LDCVs, in a sorting mechanism that occurs in vesicles, a source of bioactive peptides and thus have a role of pro-hormones.[29,30] Yet, the main function of Cgs proteins is assigned to the storage of neurotransmitters such as catecholamines.[31] Besides neurotransmitters, Cgs have the capability to entrap solutes like Ca^{2+} and H^{+}, ATP, ascorbate, biopeptides, all forming the condensed matrix in the acidic vesicle environment. The extremely low vesicle membrane conductance to H^{+} allows proton pump to maintain the secretory granule interior at a pH between 5.5-5.7.[27] This pH value is convenient for Cgs stability. Since the isoelectric point of Cg proteins is around 4.4-5.4[32] and the presence of high content of aspartic and glutamic acid residues in chromogranins, Cgs are negatively charged in secretory vesicles.[33] Catecholamines are positively charged as the pKa of the amino group is around 8.5-10. This leads to electrostatic attraction between Cgs and catecholamines and it was estimated that LDCVs can concentrate catecholamines in the concentration range from 0.5-1 M. Due to the high concentrations of different components in the vesicle, the estimated osmolarity of the interior is approximately 1,500 mOsm. However, in order to maintain vesicle equilibrium with the external environment, functional aggregation of the solutes with dense core proteins is necessary.[34]

The vesicular H^{+}-pump ATPase (V-ATPase) is responsible to maintain the pH gradient across the vesicle membrane. This is achieved by hydrolysis of ATP by the H^{+}-pump that is coupled to the movement of H^{+} into the vesicular lumen and thus the proton electrochemical gradient is created. The acidification of the vesicle lumen is not only important to the Cgs functionality and storage of ionic solutes, but is also important for the active transport of neurotransmitters into the LDCVs. This is achieved via the vesicular neurotransmitter transporter and in the case of monoamines, it is the vesicular monoamine transporter (VMAT) that uses a pH gradient to drive the uptake of one cytosolic monoamine molecule in exchange for two lumenal protons. Two distinct vesicular monoamine transporters have been identified, VMAT1 and VMAT2.[35] Endocrine

cells such as chromaffin cells in the adrenal medulla and other non-neuronal cells express VMAT1, whereas VMAT2 is present in the neurons of the central nervous system (CNS). VMAT1 and VMAT2 are responsible for the uptake of biogenic amines such as serotonin, dopamine, norephinephrine and epinephrine into vesicles; however, VMAT2 will also transport histamine.[8,36,37] VMAT2 has around a two-three fold higher affinity for most of the monoamines in comparison to VMAT1.[38] Therefore, VMAT2 is more prevalent for neurotransmitter transport during rapid vesicle recycling in the CNS, whereas VMAT1 activity is important during the slow recycling of endocrine LDCVs.[39] Since catecholamines such as dopamine produce in their oxidation reactions highly reactive quinones and free radicals, VMATs have a protective role in removal of the toxic endogenous transmitters as well.[8,40]

1.3. Chromaffin cells as models to study secretory vesicles

Studying dynamic processes at the single cell level has a great importance in understanding the complex biological systems. One of the commonly employed cell types for studies in neurochemistry and biology are the *chromaffin cells*. These are isolated from the central part of the adrenal gland, called the medulla. Cultured chromaffin cells have been used for 40 years, since the 1970s and have proved to be a good model system to study biosynthesis and storage of neurotransmitters as well as the mechanism of their release.[41,42] They have been shown to be a promising model for neuroendocrine cells and noradrenergic neurons since the structure and function of the secretory system is similar to that in neurons. In addition to secretion studies, the isolation of chromaffin LDCVs from the medulla has provided a system to understand the structure and composition of neuroendocrine secretory granules. There are two types of chromaffin cells, adrenergic (Fig. 3a) secreting dominantly epinephrine (adrenaline) and noradrenergic (Fig. 3b) releasing mostly norepinephrine (noradrenaline).[43] In the rat and human, adrenal medulla, chromaffin cells are interspersed with approximately 75% of the adrenergic cells containing enzyme phenylethanolamine-N-methyl transferase (PNMT), thereby being enable to synthesize epinephrine.[44] Both chromaffin cell types are capable of incorporating exogenous amines such as serotonin, dopamine, and norepinephrine as well as catecholamine precursors like L-3,4-dihydroxyphenylalanine (L-DOPA). They secrete the vesicle content during stimulated exocytosis with acetylcholine, Ba^{2+}, K^{+} as well as other stimuli.

In addition to primary cultures of adrenal chromaffin cells, the *PC12 cell line* (Fig. 3c) derived from a pheochromocytoma (tumor) of the rat adrenal medulla has been broadly studied as a neuronal cell model. Established in 1976 by Green and Tischler,[45] the PC12 cell line contains all the enzymes needed for synthesis, storage and release of catecholamines, mostly dopamine and some norepinephrine from LDCVs and acetylcholine contained in SLMVs.[46]

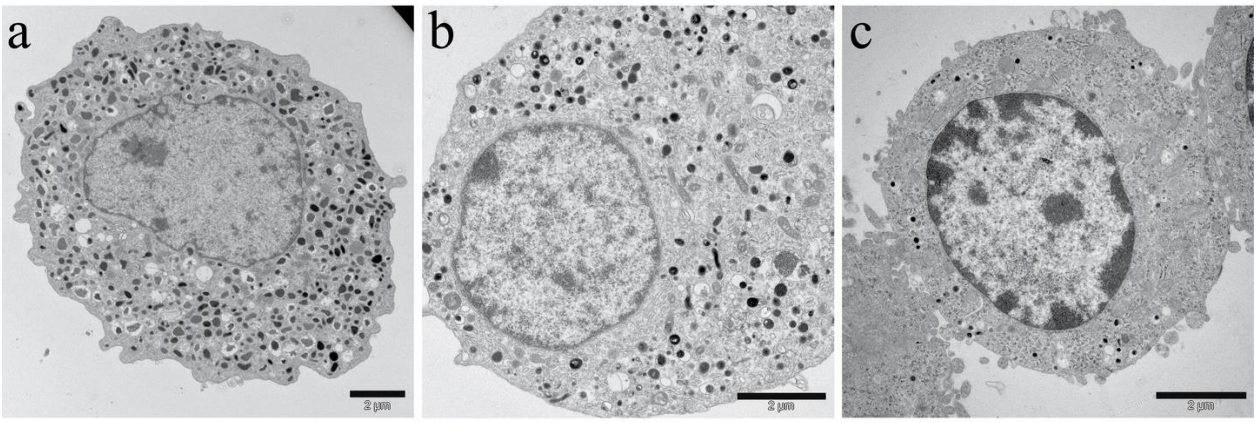

Figure 3. TEM images of chemically fixed chromaffin cells. (**a**) Adrenergic chromaffin cell; (**b**) Noradrenergic chromaffin cell; (**c**) Rat pheochromocytoma cell line (PC12). The secretory granules in chromaffin cells are distributed throughout the cytosol (**a**,**b**); however, in PC12 cells they are somewhat sporadic, mostly docked to the plasma membrane (**c**). Scale bar: 2 µm.

PC12 cells under normal conditions have morphological features, biochemistry, and physiology similar to chromaffin cells. They can differentiate in the presence of the nerve growth factor and the processes that form similar features to sympathetic neurons.[45] They undergo exocytotic release following depolarization of the cell membrane with a high concentration of K^+ or by activation of nicotinic or muscarinic acetylcholine receptors. In addition, they possess receptors coupled to G-proteins and Na^+, K^+ and Ca^{2+} channels.[47] Thus, PC12 cells have been a useful model to study neuronal differentiation, and neurotransmitter synthesis and storage as well as the functionalities of ion channels. Due to the relative simplicity of culturing and usage for a variety of studies related to the neuronal functions, chromaffin cells and the PC12 cell line are often employed in neuroscience.

1.4. An overview of biogenic amine transmitters

Biogenic amine neurotransmitters include catecholamines and serotonin, as well as the less common histamine. Catecholamines are composed of a catechol ring and a side chain containing an amino group (for the chemical structure see Chapter 4, Fig. 15.). The most dominant catecholamines synthesized in sympathetic nerves and the adrenal medulla are *dopamine*, *norepinephrine* and *epinephrine*.[48] Dopamine was discovered to be a neurotransmitter by Carlsson et al. in 1957 when they showed that it is not just a precursor of norepinephrine and has a role as a chemical messenger.[49] It plays a major role in motor control, emotions, motivation and memory formation and is involved in the etiology of several diseases such as Parkinson's disease and schizophrenia. The central norepinephrine system, in addition to cognitive functions such as attention and memory, is responsible for neuroendocrine and autonomic regulation.[50] Epinephrine has an important role in regulation of the heart rate, dilatation of the pupils and blood vessels and flight-or-fight response.

The biosynthesis of catecholamines takes place in neurons and the adrenal medulla. The synthesis in dopaminergic neurons is terminated when dopamine is produced and in adrenergic neurons at the level of norepinephrine. However, in adrenal medulla, in the presence of the enzyme PNMT, biosynthesis continues until epinephrine is the product. The biosynthesis of catecholamines starts from the amino acid L-tyrosine, which is present in the blood and can be transported through the membranes of neurons and the adrenal medulla. The enzyme tyrosine hydroxylase (TH) converts L-tyrosine to L-DOPA and is rate-limiting for the production of catecholamines. Decarboxylation of L-DOPA by aromatic amino acid decarboxylase (AADC) occurs in the cytosol of the cell with dopamine as the product. After this step, dopamine needs to be packed into the vesicles before it can be converted to norepinephrine, as the third enzyme in biosynthesis, dopamine β-hydroxylase (DBH) is bound to the inner side of the vesicle membrane. Norepinephrine is the only catecholamine produced in the secretory vesicles. The three enzymes, TH, AADC and DBH are present in both neurons and adrenal medulla. However, the last enzyme PNMT that coverts norepinephrine to epinephrine by methylation is present only in the medullary tissue. It is a cytosolic enzyme and therefore the substrate norepinephrine has to move from the vesicles to the cytoplasm to be converted to the epinephrine that will be transported back to the vesicles.[1,48,49]

After exocytosis release events, secreted catecholamines are cleared out from the extracellular space and back into the cell by a plasma membrane neurotransmitter transporter, for dopamine that is the dopamine transporter (DAT).[9,51] Hence, transported catecholamines can be loaded back into the vesicles via the VMAT or metabolized by the enzymes monoamine oxidase (MAO) and catechol-O-methyltransferase (COMT). The end products of catecholamine degradation are aromatic carboxylic acids, in humans it is predominantly homovanillic acid in the case of dopamine and for other the two catecholamines it is vanillylmandelic acid.[52] Interestingly, in rats, often used as a neuroscience model, dihydroxyphenylacetic acid is a major metabolite of dopamine as COMT is less dominant. Exogenous catecholamines that are not taken up by the cell, either diffuse away or will be degraded by COMT.[1,53]

1.5. The effect of psychoactive drugs on catecholamine storage

The storage of catecholamines and transmitter quantal size can be directly altered by administration of psychoactive drugs that have implications in treating certain neurodegenerative disorders such as Parkinson's and Huntington's diseases, psychotic symptoms and hypertension. Since Carlsson et al. showed in the experiments involving mice, that amino acid *L-DOPA*, the precursor of catecholamines is capable of passing the blood brain barrier to replenish previously depleted vesicular dopamine content,[49] L-DOPA became a target drug and today is still commonly used in the treatment of Parkinson's disease.[54,55] However, the therapy leads to end-of-dose deterioration and motor side effects like dyskinesia, thus limiting the utility of the drug. The capacity of dopaminergic neurons to synthesize, take up and store dopamine leads to a dependence on the exogenous L-DOPA that accumulates in the cytosol via the L-amino acid transporter. Typically, as long as the enzyme AADC is not saturated, L-DOPA can be efficiently converted to dopamine. The effect of exogenous L-DOPA was studied in cultured neurons,[56,57] chromaffin cells[58] and PC12 dopaminergic cell line.[25,56,59-61] It was shown that L-DOPA treatment quickly increases dopamine levels in the cytosol by more than 100-fold in some cases.[56] Moreover, Colliver et al. showed in sets of experiments on pharmacologically treated PC12 cells, that changes in the catecholamine content inside the vesicle alter the vesicle volume in a manner correlated to the amount. Thus, the concentration of neurotransmitter within the vesicles stays rather constant.[25]

Inhibition of catecholamine uptake and depletion of transmitter quantal size can be achieved by employment of VMAT blockers. One such drug commonly used starting in the 1950s is

reserpine, a *Rauwolfia* alkaloid used as an antipsychotic and antihypertensive drug. The activity of reserpine, a competitive non-transported inhibitor of VMAT,[27] was discovered by Brodie and co-workers in 1955 when spectrophotofluorometric studies showed that reserpine depletes serotonin in the brain.[62] Soon after, Arvid Carlsson suggested that the same alkaloid might have an effect on the catecholamines and he and his colleague Åke Hillarp showed in 1956 that reserpine depletes epinephrine and norepinephrine in the adrenal medulla of rabbits.[63] Even though reserpine was removed from the market due to the side effect of depression, it is still widely used in neuroscience as a pharmacological tool.

Reserpine is highly lipophilic compound that at low concentrations inhibits catecholamine influx into secretory vesicles, whereas at high dose it exhibits nonspecific detergent like behavior resulting in the direct efflux of stored transmitters.[27] The mechanism of reserpine inhibition is competitive in nature as it competes with catecholamines for the same binding place on the VMAT. It has a three-fold higher affinity for VMAT2 than VMAT1, due to the differences in substrate recognition between these two vesicle membrane transporters.[38] The binding of amine transmitters or reserpine occurs when VMAT is in the high-affinity form that is also a higher energy form. It requires translocation of one H^+ from the vesicle lumen (see section 1.2.). In this state, VMAT substrate recognition place is oriented towards the cytoplasm. When transmitter binds to the VMAT, the movement of the substrate site across the vesicle membrane occurs and it becomes exposed to the vesicle interior. The efflux of the second lumenal H^+ facilitates a VMAT conformational change and this releases the positively charged monoamine transmitter. In the case of reserpine, it has been suggested that bulky structure of reserpine restricts this VMAT conformational change. Thus, instead of releasing the substrate in the vesicle interior, VMAT becomes locked in a state from which reserpine cannot dissociate and thus prevents the translocation of the second lumenal H^+ to the cytoplasm.[35,64]

Besides reserpine, another VMAT inhibitor that is employed today is *tetrabenazine*. It is used in the treatment of hyperkinetic movement disorders such as Huntington's disease. In contrast to reserpine, tetrabenazine inhibition is affected only by high catecholamine concentration suggesting a different recognition site on the VMAT.[65] In humans, tetrabenazine has a higher affinity to VMAT2 than VMAT1, whereas in a rats, VMAT1 is unaffected by tetrabenazine treatment.[66]

2 VESICULAR MODELS – LIPOSOMES

In the 1960s it was discovered that dry lipid film upon hydration forms enclosed spherical vesicles called liposomes.[67] Since then, due to their biocompatibility and biodegradability, liposomes have found application in many areas such as nanotherapy, drug delivery, food industry, agriculture, and most importantly in this work, they have a vast application spectrum in studies of biological processes, cells, organelles and biomembranes. Liposomes are artificially prepared from lipid molecules which form a bilayer upon decrease of lipid solubility in aqueous medium (Fig. 4a-c). The main constituents of liposome membranes are phospholipid molecules. They are amphiphilic in nature, as they possess both a hydrophilic charged region, the *head group,* and the long hydrophobic *tail* (Fig. 4d). The lipid character of phospholipids originates from the long fatty acid chains that usually esterify two –OH groups of glycerol and form the tail. The fatty acid chains can differ in the degree of unsaturation and number of carbon atoms and their nature will impact the character of the phospholipid molecule. The other side of the glycerol, the last –OH group is

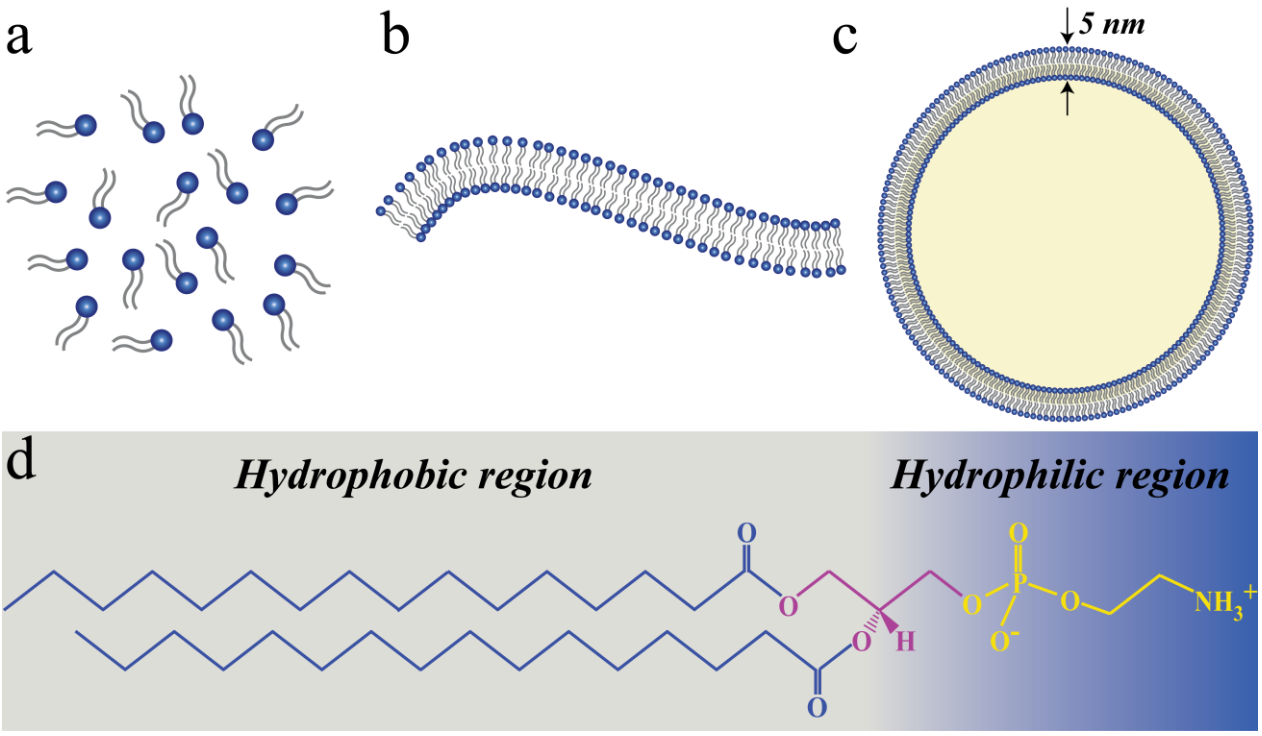

Figure 4. Schematic illustrations of liposome assembly. (**a**) Phospholipid molecules; (**b**) Leaflet of phospholipid bilayer; (**c**) Liposome with marked thickness of a lipid bilayer; (**d**) Color coded representation of phospholipid molecule, dipalmitoyl-sn-glycero-3-phosphoethanolamine (DPPE). Box colors: gray represents hydrophobic tail and blue is hydrophilic head group. In structural formula of the molecule: blue-fatty acid chains, pink-glycerol backbone, yellow-phosphate moiety attached to alcohol.

esterified with phosphoric acid, which can be further bonded to different organic molecules, preferentially alcohols like choline, ethanolamine, serine and inositol. Thus, the head group of the phospholipid molecule has the phosphate moiety along with the attached alcohol.[68-73]

Under aqueous conditions, the phospholipid amphiphilic character promotes molecule association through the weak, non-covalent bonds where the head groups orient towards the aqueous solution surrounding the membrane, whereas the tails face to the interior, away from the water. The final morphology of the liposomes depends on many factors besides the nature of the monomer building blocks. Thus, parameters of the external environment such as temperature, pH value, ionic strength or preparation methodology can influence the size and lamellarity of liposomes (Fig. 5). Based on their size, liposomes can be categorized into *small unilamellar vesicles,* SUVs ($d \leq 200$ nm), *large unilamellar vesicles,* LUVs (d=0.2–1 μm) and *giant unilamellar veiscles,* GUVs ($d \geq 1$ μm). Beside this classification, they can be distinguished based on their lamellarity as *oligolamellar*, *multilamellar,* MLVs and *multivesicular vesicles,* MVVs. In research, due to their simple preparation and well defined structure, it is preferable to use unilamellar vesicles.[68,69]

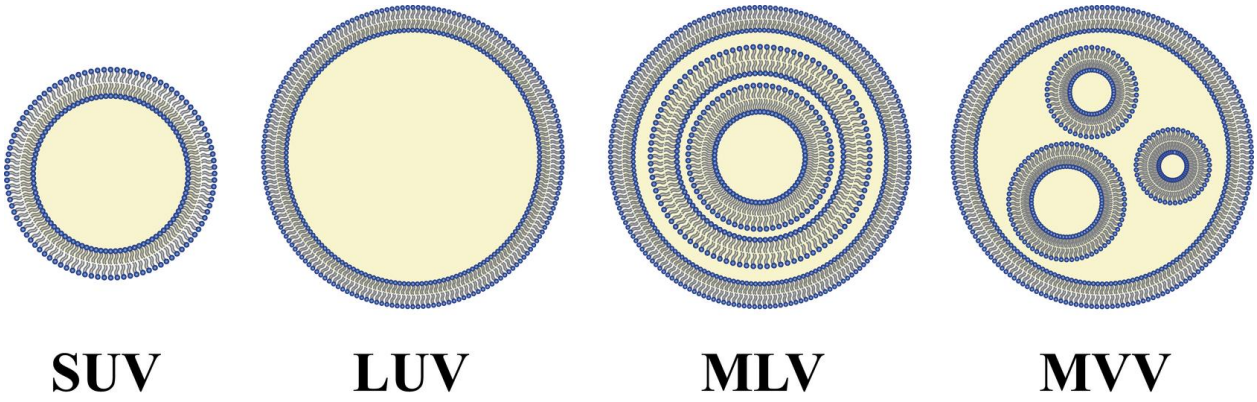

Figure 5. Liposome types based on size and lamellarity. SUV – small unilamellar vesicle; **LUV** – large unilamellar vesicle; **MLV** – multilamellar vesicle; **MVV –** multivesicular vesicle. Liposomes are not drawn to scale.

In addition to phospholipids, liposome membranes often incorporate sterol molecules. A frequently used sterol is cholesterol and it is naturally abundant in animal membranes. Cholesterol by itself does not tend to form bilayer structures, but it is capable of being integrated into a phospholipid bilayer. Thus, its –OH functional group is oriented towards the aqueous phase and the aliphatic-cyclic structure is among the tails of the phospholipid monomers. In terms of liposome science, cholesterol is used in many applications in the preparation of various liposomes to carry

certain analytes. The reason is that cholesterol tends to reduce the permeability of water soluble molecules through the lipid membrane, improves membrane fluidity, and additionally it stabilizes the liposomes especially in the presence of biological fluids such as blood, and that became very important in their application as drug delivery systems.[70,71,73]

A vast number of methodologies for liposome preparation have been developed and described in detail,[74,75] and here I describe only some of the commonly used approaches. Conventional methods include the dispersion of the lipids in the aqueous phase. Such an approach is the *Bangham method* which involves dry thin lipid film that is subjected to hydration.[67] The hydration medium might contain the analyte that has to be encapsulated. During the hydration phase, large MLVs are spontaneously formed, with low encapsulation efficiency. In order to increase the amount of encapsulated analyte of interest, the liposomal suspension might be exposed to freeze-thaw cycles that result in an increase in the loading efficiency. Due to the lack of control to obtain a certain size and lamellarity during these phases, MLVs are usually subjected to a certain type of post-processing that will allow formation of more homogenous SUVs and LUVs. This can be carried out with mechanical methods such as sonication and extrusion where the latter approach allows generation of well-defined sizes of the liposomes.[69] Sometimes it is essential to exclude the remaining un-encapsulated analyte surrounding liposomes, usually with centrifugation or dialysis. The traditional GUV preparation relies on hydration of a very thin lipid film and its swelling;[68] however, other preparation approaches have been reported.[76,77] The osmotic pressure forces triggered due to the presence of salts in the aqueous medium that is in contact with lipid film, allow lipid lamellae to detach from each other and form liposomes.[68]

The characterization of synthetized liposomes is important to understand the lipid system that will be used for experiments. Therefore, depending on the application, it is necessary to define several parameters such as stability, permeability, charge, morphology, and lastly, very often, size and concentration. The common techniques to measure particle size and size distribution are dynamic light scattering (DLS) and nanoparticle tracking analysis (NTA). Both techniques rely on the Brownian motion that the particles of interest experience and light scattering. In the case of NTA, particles in suspension can be visualized as laser light that is passed through the sample is scattered by the particles that are present. Each particle is tracked by the software and by applying the Stokes-Einstein equation it is possible to calculate particle diameter.[69] NTA has the capability to measure particle sizes between 0.03 and 1 μm, and that should be sufficient for SUVs and LUVs size characterization. An important extra feature that NTA provides is concentration measurement,

where concentration is expressed as the number of particles per volume. In the case of GUV for size measurements, light microscopy is often employed.

2.1. Liposomes containing an aqueous two-phase system

Living cells are crowded systems of macromolecules, cytoskeletal network and variety of organelles. The common phenomenon that involves separation of certain cytoplasmic regions without the presence of a clear barrier is called micro-compartmentalization.[78,79] The process of compartmentalization is essential for cell function but, even today, its mechanism is not clearly understood. However, some of the mechanistic views have been proposed such as phase separation where cellular metabolites are subjected to compartmentalization as a result of their partitioning between phases.[79]

To study and characterize such a process, the living cellular system is extremely complicated. Thus, as a bottom up approach has been used, where different methodologies have been developed to synthesize artificial models for cells or organelles. Compartmentalization of nucleic acids via metabolic buffering[80] or proteins that partition between two polymer aqueous phases[81] have been reported. The basic principle in the latter example relies on a phase separation of polymer mixtures due to their high molecular weight and certain molecular interactions.[82] This system, called an *aqueous two-phase system* (ATPS), has been heavily employed to mimic the compartmentalization processes at the cellular and sub-cellular levels. The method of encapsulating ATPS within giant unilamellar vesicles as a model for cell or organelle function was developed by the Keating group.[83] In **Paper III**, ATPS was employed to mimic the internal morphology of LDCVs, the dense core and halo. There is a large range of macromolecules that can be applied in making an ATPS; however, the well characterized polymers, dextran and polyethylene glycol (PEG), are frequently employed. They are mixed at concentration above a few weight percent in each polymer and the desired amount can be estimated based on their phase diagrams.[84] Commonly, encapsulation of the ATPS is done during the swelling phase of GUV preparation. A dry thin lipid film is subjected to warm, homogenous aqueous solution that contains the macromolecules that will form the ATPS. Later cooling of the system will initiate phase separation of polymers within GUV. Separation of the macromolecules is reversible, thus subsequent temperature increase or changes in osmolality of the surrounding solution will again trigger polymer mixing. In Figure 6a, a liposome-ATPS system is shown where dextran is partitioned in the inner region of the GUV, while PEG is

partitioned in the vicinity of the lipid bilayer. This was confirmed with fluorescence imaging by use of a fluorophore conjugated with dextran showing its localization in the central part of the GUV (Fig. 6c).[85]

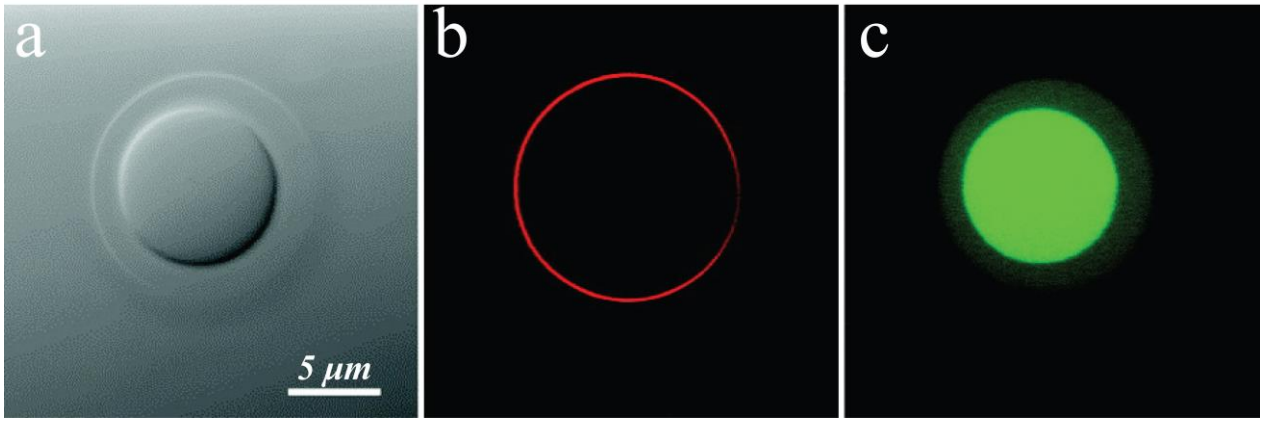

Figure 6. Two-compartment GUV containing PEG-dextran ATPS imaged with confocal microscopy. (**a**) Encapsulation of ATPS, where dextran phase occupies inner part of the GUV and PEG is external phase; (**b**) Rh-DOPE fluorescence signal showing unilamellarity of GUV; (**c**) Alexa488-dextran fluorescence proving that dextran is phase separated from PEG and localized the most inner of GUV. Rh- DOPE - 1,2-dioleoyl-sn-glycero-3-phosphoethanolamine-N-(lissamine rhodamine B sulfonyl). Adapted with permission from the reference.[85]

At the bulk level, heavier dextran partitions below the PEG phase owing to the force of gravity. Thus, it seems evident that the PEG phase should always occupy the inner space of the liposome interior. However, in a microvolume, the gravity effect is less profound and surface interactions can be more dominant. Thus, it is possible to change the localization of the phases by having the PEG phase wet the liposome membrane and then the dextran phase will be in center of the liposome.[78]

The reductionist approach using synthetic cells and organelles is clearly an approximation and a model for some aspects of cellular function. If phase separation happens in living cells, thousands of molecules would compartmentalize resulting in a large number of different phases. They would be located within the cell based on the strength of intermolecular bonds. It is obvious that this is not the case in a living cell. However, the simplicity of the synthetic systems such as ATPS within liposomes has the benefit of allowing understanding the mechanism of micro-compartmentalization during processes of protein folding or DNA condensation.

2.2. Peptide conjugated liposomes

Numerous surface modifications of liposomes have emerged from experiments aimed at using lipid vesicles as drug delivery systems. Different ligands and receptors have been employed to decorate liposomes that are unique in order to target specific cells and tissues. Thus, proteins such as antibodies, vitamins, hormones and others have been used to make liposomes suitable for their introduction into biological systems and to target specific chemical interactions.[72] After the binding phase of liposomes to the cell surface and their endocytosis, lysosomal degradation takes place and the eventual fate of the encapsulated macromolecules is unpredictable. It has been suggested that the endocytosis phase could be avoided by creating a liposomal surface modification with peptides that have the ability to directly penetrate through the cell membrane.[86,87]

The first peptide that has been employed for liposome membrane penetration was peptide derived from human immunodeficiency virus-type 1 (TAT) consisting of six arginine and two lysine residues.[87] Due to the high arginine content in the TAT sequence, Futaki's research group synthesized polypeptide molecules having only arginine residues.[88,89] They concluded that the arginine octamer (R8) was the most efficient for cellular internalization.

There are a few coupling methods to bind the peptide to the liposomal membrane. It was shown that peptides can be directly attached to the liposomal surface.[87] However, an amphiphilic linker that is conjugated to peptide can also be employed as an anchor to the hydrophobic carrier such as a liposome (Fig. 7).[90] Torchilin et al. showed that it is possible to use a spacer, *p*-nitrophenylcarbonyl-polyethylene glycol, that is attached to a hydrophobic phosphatidyl ethanolamine to couple to the TAT peptide (TATp-PEG-PE).[87] Another approach to link liposomes with peptides was reported where the spacer and hydrophobic anchor was stearic acid. Several stearylated arginine-rich peptides were synthesized and became a new class of molecules suitable for transfection.[91] It was shown that stearylated octamer of arginine (STR8) had the best efficiency in cellular uptake. Continuing with this carboxylic acid-peptide idea, Iwasa et al. used STR8 in order to employ a stearyl moiety as a linker between octaarginine and lipid vesicle (Fig 7).[92]

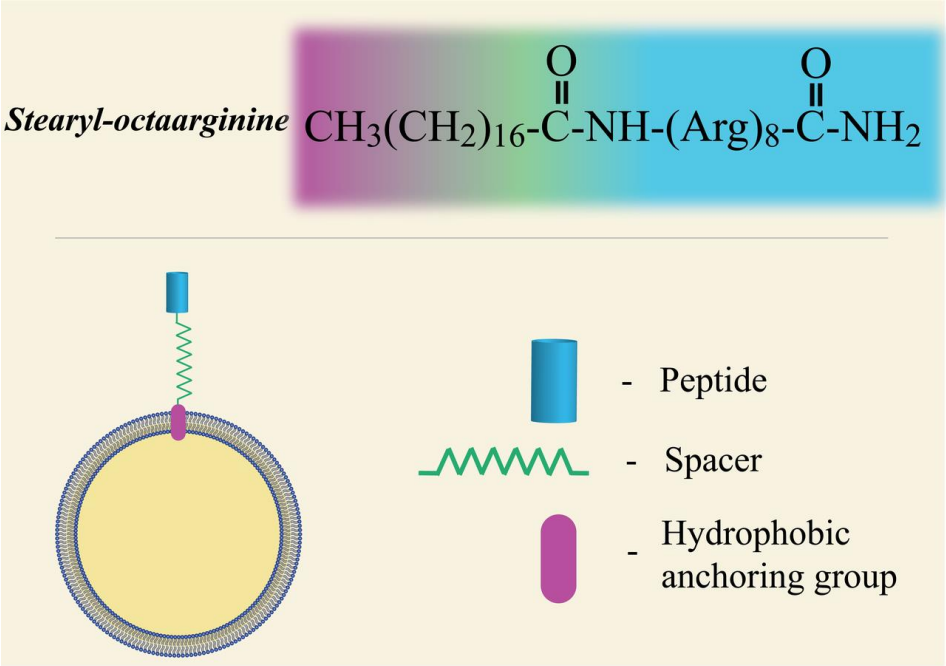

Figure 7. Peptide attachment to a nanocarrier (liposome). The role of the spacer is to bridge between the hydrophobic moiety (membrane) and the peptide molecule. In the case of stearylated peptide, the hydrophobic chain originating from the carboxylic acid has a double role, to anchor the peptide into the liposome membrane and as a spacer. STR8 molecule (top) is color coded with the colors of principal components (bellow). Structures bellow are not drawn to scale.

In this thesis, I employed stearylated octaarginine coupled to liposomes as a simplistic bottom up approach to introduce a protein-like nature to the membrane. This was important in the study described in **Paper II**, where I worked towards understanding the role of membrane proteins in the rupture mechanism of native vesicles onto an electrode surface.

3 ELECTRON MICROSCOPY TECHNIQUES

Development of the light microscope in the late 16th century by Dutch spectacle-makers, Hans and Zacharias Janssen, and almost a century after, the application of the light microscope to describe biological specimens by Hooke and van Leeuwenhoek, opened a door to the important advancements in biological and life sciences today.[93] Even though the affinity based labeling has led to imaging at the subcellular level, conventional light microscopy is limited by the wavelength of light and thus two objects cannot be distinguished when they are closer than ~ 200 nm in the X-Y plane and ~ 500 nm in Z direction.[94] Application of light with shorter wavelength, such as UV light, introduces improvements in spatial resolution but only down to ~ 100 nm.[95] In the 1930s, the first electron microscope (EM) was developed and by taking the advantage of the shorter wavelength of electrons it became possible to dive into the submicroscopic world and gain a better understanding of cell and tissue organization. The basic difference between light and electron microscopes is that the latter uses an accelerated electron beam for illumination instead of visible light and a coil-shaped electromagnet as a lens to shape the electron beam. Nowadays, electron microscopes can reach spatial resolution down to ~ 1 Å, 4,000 times better than conventional light microscopes. Their resolving power is determined by the beam voltage, lens aberration and aperture size. Even though electron microscopes offer excellent resolution capabilities and have found a wide range of application, their biggest disadvantages are the sampling, instrumental cost, sample preparation, interpretation of results, and electron beam damage that might influence EM applicability in imaging live samples.[96,97]

In this thesis, in **Papers IV** and **V**, two types of electron microscopy have been employed, *transmission electron microscopy* (TEM) and *scanning electron microscopy* (SEM) to image the morphology of subcellular features in neuroendocrine cells as a complementary approach to SIMS imaging.

3.1. Transmission electron microscopy

TEM has been widely employed to study the finest structural features of cells and cellular fractions, tissues, and other biological specimens. In past decades, much effort has been invested to develop this microscopic technique and improve the resolution of imaging. The main components that comprise the TEM instrument are an electron optical column, vacuum, and electronic systems. The electron optical column (Fig. 8) has an integrated electron gun with its electron source (tungsten, lanthanum hexaboride or field emission gun) with a brightness that defines the imagining capabilities, including resolution. The electron beam is focused onto a very thin slice of specimen by use of condenser lenses. Further, the objective lens system forms the two-dimensional image, which is magnified and projected by projector lenses onto a viewing device such as fluorescent screen or CCD camera. The number of electrons that are transmitted through the sample is proportional to the brightness of the certain area of the specimen. The electron optical column is evacuated with a vacuum pump system to enhance the mean free path of electrons and avoid collisions with molecules from the environment. This allows the wave nature of electrons to be used to image with high-spatial resolution. Electrons can only be transmitted through a very thin sample, thus sample preparation methodology of water rich samples such as biological specimens needs to include some type of fixation and consequent sectioning.[96,97]

3.2. Scanning electron microscopy

SEM has found its application in biological sciences as well, owing to its capability for obtaining surface images with a magnification range of 10-10,000 × and resolution practically the same as the spot size of a focused electron beam. Figure 8. shows the basic principle of operation for SEM. Similar to TEM, in SEM, an electron beam is formed by a source such as tungsten filament or field emission gun and it is passed through a system of apertures and condenser lenses that shape the electron beam to a nanometer beam spot. The surface of the sample is scanned by the beam by use of scanning coils that raster the electron beam over a rectangular area on the sample surface. Finally, fine focusing is achieved by objective lenses just before the beam hits the sample. While the beam is interacting with the sample surface, different types of signals are formed, such as secondary and backscattered electrons, that are used for topographic analysis and X-rays suitable to characterize the sample composition. Except for environmental SEM, that can operate

at pressures as high as 50 Torr and image wet, dirty and oily types of samples, conventional SEM instruments operate in a high vacuum environment and thus biological sample preparation methodology in an important consideration.[96,98]

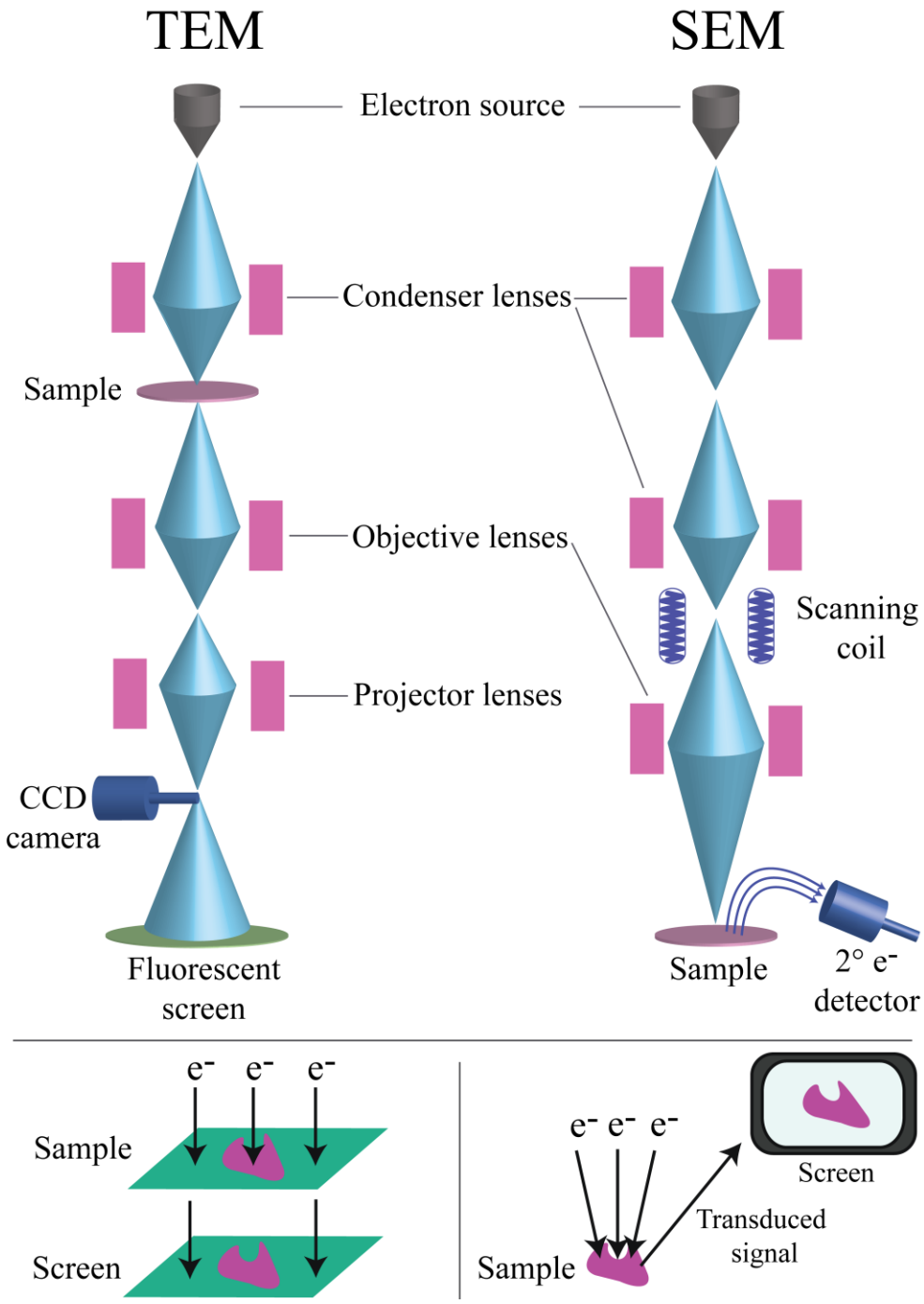

Figure 8. Schematic representation of the operation principles for TEM and SEM. Both electron microscopes contain four parts: electron source, electromagnetic lens system, sample holder, and imaging system.

3.3. Sample preparation of biological specimens for electron microscopy

As mentioned in previous sections, biological samples, such as cells and tissues, contain a large amount of water and therefore they require complex sample preparation procedures for electron microscopy analysis. This is especially true for TEM imaging, as sample preparation is quite complicated and composed of several steps.

TEM sample preparation methodology covers a wide range of approaches and the choice of method depends on different factors such as sample type, the study that will be carried out, infrastructure available, etc. The most crucial phase of sample preparation is the fixation process in order to preserve three-dimensional features of biological samples. There are two main ways to preserve shape and internal morphology, by chemical fixation and cryo-fixation. *Chemical fixation* has been widely used since the 1940s with the introduction of osmium tetroxide as an agent for fixation and staining[99,100] and involves aldehydes as initial fixation agents which application started during 1960s.[101] In the most common chemical fixation methodologies, biological samples are first fixed with aldehydes and this phase is called the initial or primary fixation. Aldehydes, such as formaldehyde and glutaraldehyde, cross-link proteins by means of forming a Schiff base with the protein amino groups and could be efficient fixatives for certain types of lipids. Post-fixation and staining with OsO_4 follows the initial fixation, and here the OsO_4 has a role to immobilize lipids, mainly unsaturated ones. In order to prepare the sample for ultrathin sectioning (below 100 nm), the specimen has to be embedded in plastic resin. As resins are hydrophobic, a dehydration step is necessary prior to resin exposure and embedding. This is achieved by exchanging water content with ascending concentrations of organic solvents such as ethanol and acetone. After infiltration with resin, samples are cured either with heat or UV light, depending on the resin type. Thin sectioning is performed with an ultramicrotome and after post-staining sections with salts of heavy metals, such as uranyl acetate or lead citrate, they can be used for TEM analysis. Currently, chemical fixation has a wide range of applications; however, it has some disadvantages as well, which can in some cases impact the interpretation of the results and limit the sub-angstrom resolution of the TEM. Fixation with aldehydes has a gradient penetration that can cause the interior of the sample to be relatively unfixed. Moreover, lipids can retain mobility after fixation and be extracted during the dehydration and embedding steps. Additionally, there is a danger of redistribution and loss of small molecules and ions.[102] A newer approach for fixation, *cryo-fixation*, was developed during the late 1970s. In comparison to chemical fixation, this approach has goals

to avoid loss of small molecules and to preserve sample morphology by means of more controlled exposure to chemical fixatives, if used, and more gentle dehydration and embedding steps. There are many ways to perform cryo-fixation, and the basic concept includes rapid freezing and preparation for imaging. Rapid freezing allows one to immobilize and preserve sample morphology without ice crystal formation, where vitrification is necessary. Depending on sample size, freezing can be performed as plunge freezing for the small sample size (viruses, single cells etc.), slam freezing (thickness of the sample can be maximum 20 μm) and high-pressure freezing (HPF), for samples up to 200 μm thick. Frozen samples or their cryo-sections can be directly observed with cryo-TEM. However, in the case where imaging should take place at room temperature, further preparation should be done. This is possible with freeze substitution (FS), that involves dehydration at a low temperature (-90ºC) when the viscosity of organic solvents increases, thus limiting protein mobilization, and stabilizing the sample. Staining with heavy metal salts, embedding in plastic resin, and its polymerization at low temperatures are the following steps in FS. If it is necessary, fixatives such as aldehydes and OsO_4 can be added to the FS cocktail, especially if embedding and polymerization will be done at room temperature. Even though cryo-fixation is becoming a more popular fixation approach today, it has several disadvantages as well, such as the demand for sample size and investment in necessary equipment (eg. HPF and FS systems).[103-105]

Water rich biological samples have to be preserved for high-vacuum SEM analysis and thus sample preparation methodologies have been developed. As in a case of TEM, here samples also have to be fixed and dehydrated. Fixation with aldehydes and dehydration with organic solvents can be done at room or low temperatures. Organic solvents can be dried on air or by freeze-drying. However, during this phase, artifacts could happen due to the sample shrinkage and it's collapsing. This can be overcome with an approach called critical point drying, where at high pressure, organic solvents like ethanol are replaced with transitional fluid or liquid carbon dioxide. Transitional fluid or gas, is removed in its supercritical state where no gas-liquid interface exists protecting the architecture of the specimen. Finally, in all these preparation schemes, owing to the low conductivity of biological specimens, electrical charging might occur from the electron beam impacts, and this can interfere with both the subsequent primary beam and emission of secondary electrons. Therefore, the specimen should be coated by sputtering of ultra-thin layer of metal such as Au, Pt, Ag, Ir or by thermal evaporation of carbon.[98,106,107]

4 ADVANCED NANOANALYTICAL TOOLS TO STUDY TRANSMITTER VESICLES AND LIPOSOME MODEL SYSTEMS

In this chapter, the techniques that have been employed to chemically image at subcellular level and measure the neurotransmitter content at nanometer scale are described and discussed. In **Paper III**, time-of-flight secondary ion mass spectrometry (ToF-SIMS) was used to probe the content of two different liposome systems that were used to mimic native vesicles. Further, ToF-SIMS was applied as a discovery tool in advancing the flow of ultrahigh resolution imaging, such as NanoSIMS and this is discussed in **Paper IV**. The latter SIMS technique was used to image the dopamine content in LDCVs in **Paper V** and proved to be a good assay tool for screening vesicle storage dynamics in neuroendocrine cells. In addition to imaging approaches, electrochemical techniques were also employed, such as single cell amperometry and a novel method called vesicle electrochemical cytometry, to quantify and compare the neurotransmitter content present in liposomes and neuroendocrine vesicles of chromaffin and PC12 cells. This work is presented in **Papers I**, **II** and **V**.

4.1. Imaging mass spectrometry

The drive to understand chemical processes and reveal intricate structures in complex biological samples has allowed us to gain new imaging information that was not possible with previously heavily employed microscopy techniques. The search for localization of various chemical species, simultaneously, that are difficult with light microscopy approaches has led to the idea to employ *imaging mass spectrometry* (IMS) techniques. The ability of IMS to localize large biomolecules, small molecules, and their fragments, atoms, and isotopes with sufficient lateral resolution to look at tissues, cells and organelles, makes this imaging approach very attractive in the fields of chemistry, biology, pharmacology, physics, and others. Additionally, by improving the resolution capabilities, sensitivity and the mass range, IMS is leading to improve studies at cellular and sub-cellular level. The process of mass spectrometry imaging can be basically divided into few steps. Appropriate sample preparation, especially in the case of delicate biological samples is the critical first step. Desorption of the analytes and their consequent ionization follows.

Separation of charged species in a masses analyzer based on their masses and acquisition of images that will be further processed is the final step in this process. Two IMS techniques frequently employed in the analysis of biological specimens that differ significantly in desorption and ionization processes are *matrix-assisted laser desorption/ionization* (MALDI) technique and *secondary ion mass spectrometry* (SIMS).

The MALDI technique, first developed by M. Karas et al.[108] in 1985, is a label-free mass spectrometry imaging approach that maps biomolecular ions and is mostly used for species with high molecular weight. Application of a high-energy pulsed laser beam in combination with a suitable light adsorbing matrix makes MALDI a soft ionization technique with the ability to image, in parallel, intact peptides, proteins and lipids.[109,110] However, despite the capability of MALDI to chemically image large biomolecules, its application in the analysis of biological samples is restricted. Due to its limitation in spatial resolution, as only focusing of the laser beam to about a 1-2 µm spot size can be achieved at best, and as further resolution improvement would reduce the sensitivity, sub-cellular imaging is extremely challenging.[109,111]

Another IMS technique that is broadly applied in biology is SIMS. As well as MALDI, it is capable to analyze complex samples owing to the chemical precision allowed by mass spectra acquisition.[110,112,113] In SIMS analysis (Fig. 9), a focused primary ion beam is used to sputter away the material from a sample.

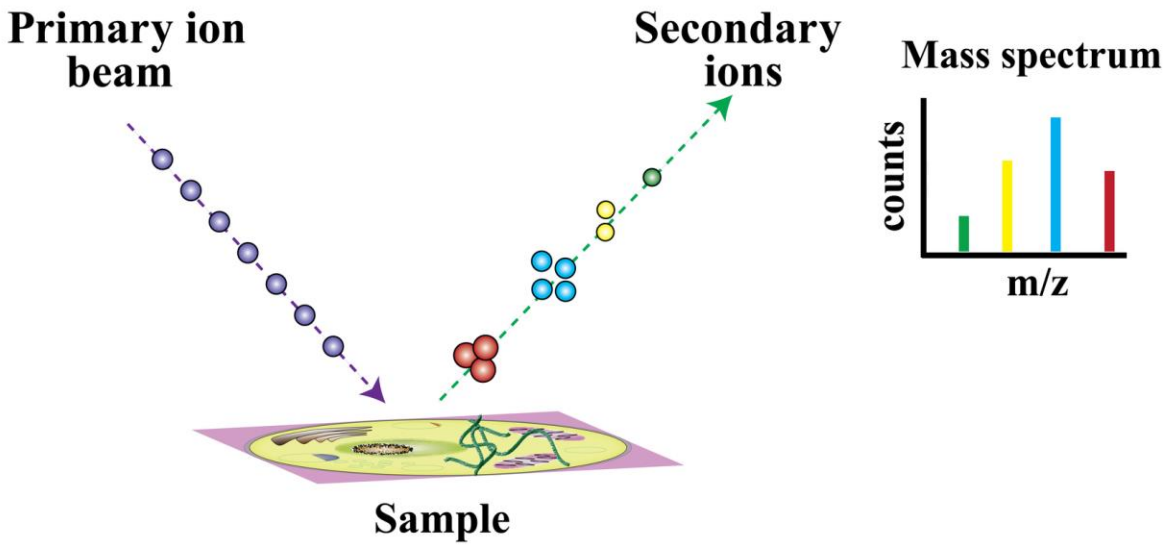

Figure 9. Schematic representation of the SIMS process. The primary ion beam is focused on the sample surface and sputters away secondary particles. Only a small fraction of the sputtered particles are charged forming secondary ions. By measuring the mass-to-charge ratio of secondary ions and detecting the counts of each charged species, mass spectrum can be acquired for each image pixel.

The primary ion beam in SIMS is focused on the sample and secondary species, which can be neutrals, electrons and ions, are sputtered from the surface. Approximately 1% of all secondary particles are charged and they are extracted into the mass spectrometer to be analyzed resulting in a mass spectrum.[112,114-116] High-energy primary ion beams can be focused with great precision; however, this results in fragmentation of the molecules that are analyzed. Therefore, SIMS analysis provides high-spatial resolution imaging of a variety of biomolecules over a mass range up to 1,000−1,500 Da,[117] but often the species above about 300 Da are fragmented in static SIMS and atomic species are observed in dynamic SIMS described below. Depending on the charge, size, and current of the primary ions, it is possible to focus the ion beam that impinges the sample surface, down to 40 nm in a method called NanoSIMS.[112,118-120]

Sputtering is a damaging process; therefore, to avoid collecting data from a damaged area, it is important to know how much of the surface is impacted by the primary ion. In order to collect mass spectra from surface what is called the static mode (relatively unchanged surface), a criterion called the static limit has to be met. Here, the primary ion dose should be below ~10^{-13} ions/cm^2.[114,121,122] This method is called *static* SIMS and allows better collection of molecular ions and less surface damage than dynamic SIMS. However, the major challenge for the static SIMS is sensitivity, especially in the case of the lower concentrations and complex samples. If the primary ion dose is above the static limit, when the number of incident primary ions exceeds the number of the surface atoms on a sample, SIMS is called *dynamic*. Due to the high level of fragmentation and erosion, dynamic SIMS provides elemental information with high count rates in small pixels and consequently it is more suitable for subcellular studies, localization of isotopically labeled molecules, and three dimensional imaging.[116,123,124]

In static SIMS, the primary ion beam that has energy typically between 5 and 40 keV bombards the surface of interest and the energy is transferred to the analyzed material. This process is called the *collision cascade* and is similar to the collision of the billiard balls in a pool game.[114] The bond energy of most molecules existing in a sample (covalent, metallic and ionic) are typically in the range of 1-10 eV/bond,[125] and this is much lower than the energy of the projectile species. Thus, in a proximity to the collision site extensive fragmentation occurs and mostly atomic secondary species are formed. Further from the collision epicenter, approximately 5-10 nm, less fragmentation is observed and it is possible that intact molecules are sputtered.[110,114,117]

Performing the SIMS experiment properly necessitates a basic knowledge about *primary ion sources* and what chemical information and spatial resolution they can provide. Energetic primary

ions cannot desorb fragile organic molecules without fragmentation. Application of the liquid metal ion sources, such as indium or gallium first opened the door to the high-spatial resolution imaging of organic molecules. However, they provided a poor yield of high-mass secondary ions and thus the identification of the original molecules was complicated.[126,127] The imaging in a high-spatial resolution mode, the NanoSIMS modality, requires the use of the high energy Cs^+, O^- or O_2^+ ion probe beams that can be focused to a spot size of several tens of nanometers. This process results in high secondary ion yields but the drawback is a high level of fragmentation. Thus, to obtain molecular information from the sample surface, molecules of interest are usually isotopically labeled.[124,128,129] In static SIMS, the discovery of the non-linearity in the increase of the secondary ion yields as a function of a particle nuclearity,[130] has led to the search and development of cluster primary ion beams that have overcome the sensitivity issues in imaging molecular ion species. Cluster ion probes such as Bi_n^+,[131] C_{60}^+,[132] Ar_n^+,[133] offer much better ability to desorb molecular ions without extensively damaging the sample surface. The use of large cluster ions such as C_{60}^+ and Ar_n^+ enhances the yield of high mass molecular ion species, minimizes the damage to the subsurface and thus enables molecular depth profiling to be possible as well. However, because of the difficulty to focus them, spatial resolution has not yet approached that needed for many subcellular analyses and not that of NanoSIMS.

SIMS experiments, especially imaging (more below), demand high repetition rates for sampling, thus only a few *mass analyzers* are fast enough. In addition, the requirements for static or dynamic SIMS also impact the choice of mass analyzer. Today, the most employed mass analyzers in SIMS are the quadrupole mass filter,[134] the time-of-flight (TOF),[135] and the magnetic sector.[136] Owing to their small size and easy incorporation into the ultra-high vacuum environment used for analysis, quadrupole mass filters were frequently employed during the beginning of the SIMS era. However, the transmission capability for quadrupole mass filters is below 1% leading to high information loss in the mass-scanning mode. Dynamic SIMS is usually performed with a magnetic sector analyzer due to its high mass resolution and high transmission. As a scanning device, it functions well in a combination with a continuous primary ion beam and has led to the high-resolution SIMS instrument, or NanoSIMS. Lastly, high transmission TOF mass analyzers with high sensitivity are traditionally applied for molecular SIMS, especially for imaging (see below), owing to the capability to collect all or most secondary ions produced, operating in quasi-parallel mass filtering mode.[114,115]

4.1.1. Time-of-flight SIMS imaging

ToF-SIMS is a versatile technique that has found application in different areas of research in academics and industry. It is a highly sensitive technique that reveals the molecular and chemical information with a low detection limit and high-spatial resolution. Consequently, this technique has been frequently used for the analysis of polymers,[137] metals,[138] and perhaps most importantly, complex biological samples.[139-144]

In ToF-SIMS, a pulsed primary ion beam is impinged on the sample surface and generates the secondary ions, which are subsequently extracted by a high energy voltage via the extractor, into the TOF mass filter (Fig. 10).

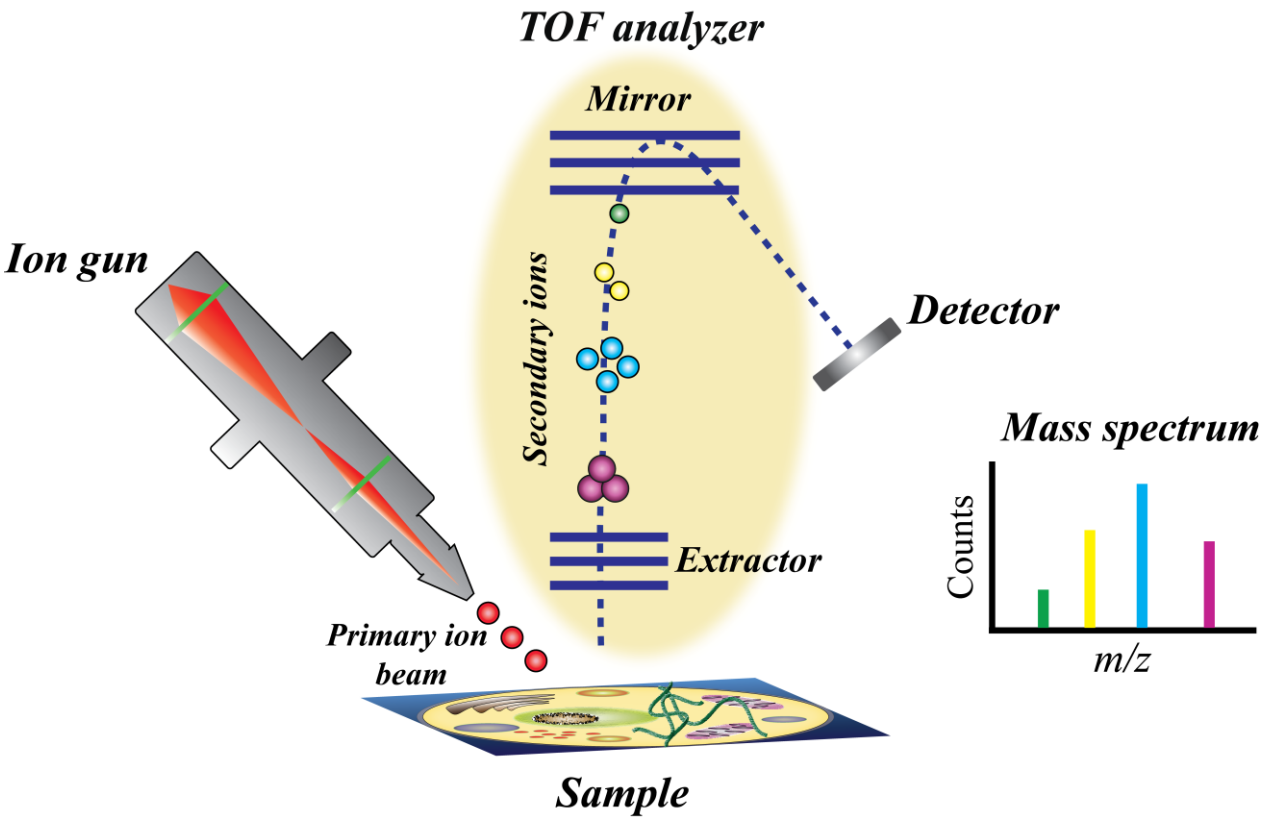

Figure 10. Schematic representation of the ToF-SIMS. A focused, pulsed primary ion beam is used to raster over the sample surface and dislodges secondary ions. Generated secondary ion species are accelerated and on a way to the detector, they enter into the TOF mass analyzer where the particle separation occurs based on the time-of-flight through the analyzer. ToF-SIMS allows recording of a mass spectrum at each pixel for known and unknown ion species and therefore represents a tool for a label-free analysis.

The time-of-flight of extracted secondary ions from the sample to the detector is used to generate a mass spectrum at each pixel for known and unknown ion species. The basic principle of TOF mass analysis relies on the secondary ions having the same kinetic energy from acceleration of the secondary ions at a potential of several keV. In the TOF tube, which is field-free space, the accelerated secondary ions drift until they reach the detector. Separation is dependent on their mass over charge ratio (*m/z*) as at the same kinetic energy, lighter ions travel faster and vice versa. By relating the travel times to ion masses, a mass spectrum can be constructed from the each point of the sample surface that is analyzed.[114,145]

Pulsed primary ion beams used with TOF analyzers for SIMS analysis allow several interesting features. One of these is that efficient *depth profiling* in the static SIMS mode is possible. In addition to the primary ion probe for surface analysis, another ion gun, operating in an interlaced mode, can be employed to etch away the damaged surface that was imaged with the analysis beam. For etching purposes, a projectile with a high sputtering rate, low damage and low penetration depth can be employed such as the C_{60}^+ or SF_5^+ ion probes.[146,147] Pulsing the primary ion beam additionally allows effective charge compensation in analysis of non-conductive samples by employing a pulsed low-energy electron flood gun. While charge compensation by the current from the electrons has had many useful applications, one should also take into account the surface damage by the impinged electrons and thereby other compensation approaches might be considered.[114,148,149]

When the pulsing mode is employed during primary ion beam operation, the pulse time length impacts the *mass resolution*. The rule of thumb is that higher mass resolution is obtained if the pulse width is shorter. If the initial pulse is bunched into very narrow pulses (several hundreds of picoseconds), then higher mass resolution is obtained ($m/\Delta m > 8{,}000$), although the spatial resolution is then degraded (several μm). The mass resolution is also poorer if secondary ions sputtered from the sample surface have a wide energy distribution or are accelerated into the TOF analyzer from different distances from the surface. Here, secondary ion species with the same mass will have different velocities and thus arrive at detector at different times that will degrade the mass resolution. This can be overcome by introducing an ion mirror (Fig. 10) in the TOF tube that allows more energetic ions to penetrate longer and contrariwise so that the ions have a more narrow energy distribution when they are reflected out.[114] Additionally, topography of the sample should be also considered, as the secondary ions emitted from different heights may be shifted, and this will lead to lower mass resolution.[150] Higher *spatial resolution* can be achieved in the non-bunched mode of

the TOF.SIMS instrument (ION-TOF, GmbH) by prolonging the pulse duration (tens of nanoseconds) in order to better focus the primary ion beam and achieve sub-micron resolution. However, this decreases the mass resolution as the peaks in the mass spectrum become wider.[112,145]

The environment of the analyzed material can also effect the ionization probability of the analyzed species. This phenomenon of secondary ion emission dependence upon the chemical and electric environment is called the *matrix effect*.[114,151,152] Thus, the matrix effect has to be considered in the experiment design and in data interpretation. In order to be able to correlate the analyte concentration with the fluctuations of the ion intensity, it is of vital importance to keep ionization efficiency constant across the analyzed sample, if possible.

Since SIMS instruments operate in an ultra-high vacuum (UHV) environment, the *sample preparation* of biological specimens is essential for obtaining successful and meaningful information, especially if the goal is high-spatial resolution image acquisition. It is important to preserve not only the native distribution of the molecules of interest, but also to maintain the inner morphology of the sample, mainly for the 3-dimensional chemical imaging. There are many protocols that have been developed for specimen preparation, and depending on the aim of the imaging experiments they need to be chosen accordingly. Commonly employed protocols are chemical fixation, drying at room temperature, freeze-drying, freezing while maintain inner water (frozen-hydrated and freeze-fracture).[153-156] Freezing samples has typically led to the best sample preservation methodology, especially the frozen-hydrated approach. With this methodology, cells or tissue are frozen quickly (plunge-freezing) usually in liquid propane, ethane or isopentane. The rapid conduction of the heat from the sample allows the process of vitrification, the formation of non-crystaline amorphous ice instead of crystalline ice that can damage the sample.[154] Frozen samples can be fractured inside the SIMS instrument under UHV conditions and thus they will not be contaminated from the environment. Additionally, fracturing can make the sample more available for analysis by exposing the inside of tissues and cells, an important gain for cellular and sub-cellular imaging.[157]

4.1.2. Magnetic sector SIMS imaging – NanoSIMS

A propitious technique for high-resolution chemical imaging that provides higher secondary ion yields in a comparison with ToF-SIMS is magnetic sector SIMS. One of the commercial versions of the magnetic sector SIMS existing today are the Cameca NanoSIMS 50 or 50L instruments.

NanoSIMS uses a scanning ion microprobe that operates in the dynamic SIMS mode (Fig. 11). It has the capability to analyze most of the elements in the periodic table with sub-micrometer lateral resolution. *Primary ion sources* available are either the cesium positive ion source or the oxygen negative ion source that can be either a duoplasmatron or radio frequency (rf) plasma source. The cesium primary ion beam generates negative secondary ions and can be focused down to 30-50 nm, whereas the oxygen primary ion beam favors formation of the positive secondary ions.[118-120,128] Depending on the type of oxygen source, different spatial resolution can be achieved. The duoplasmatron source can reach a beam diameter of about 150 nm,[119] while the rf plasma source has a 40 nm diameter beam that is comparable to the spatial resolution of the Cs^+ primary ion source.[128] High energy primary ion bombardment leads to breakage of molecular bonds in the sample, thus generating mostly monoatomic and diatomic secondary ions. Therefore, molecules of interest must either have a specific element to detect or be isotopically labeled. Secondary ions that are sputtered from the sample surface are separated according to their mass-to-charge ratio (*m/z*) in a dual-focusing sector mass analyzer, first with an electrostatic filter and then further with a magnetic sector. The double focusing capability of the mass spectrometer allows the NanoSIMS instrument to image with a high-mass resolution of several thousand. This is sufficient to resolve the isobaric interferences of elements with low atomic numbers. The instrument does not scan the masses, but has several positional detectors. Thus, unlike ToF-SIMS, the Cameca NanoSIMS can detect only up to 7 species simultaneously as it has this many electron multiplier detectors and Faraday cup.[112,118]

The unique feature of the NanoSIMS instrument is the use of *coaxial ion optics*, which allow co-propagation of primary and secondary ions. This design enables the ion optics to be close and perpendicular to the sample. Therefore, the primary ion beam spot size can be reduced and the lateral resolution and the secondary ion collection efficiency (transmission) are improved. Because of the coaxial design of the optics, the primary and secondary ions must be of opposite polarities.

The NanoSIMS imaging technique has proven to be useful in a wide range of research fields such as material science,[158] biological geochemistry and cosmochemistry,[118] plant research,[159]

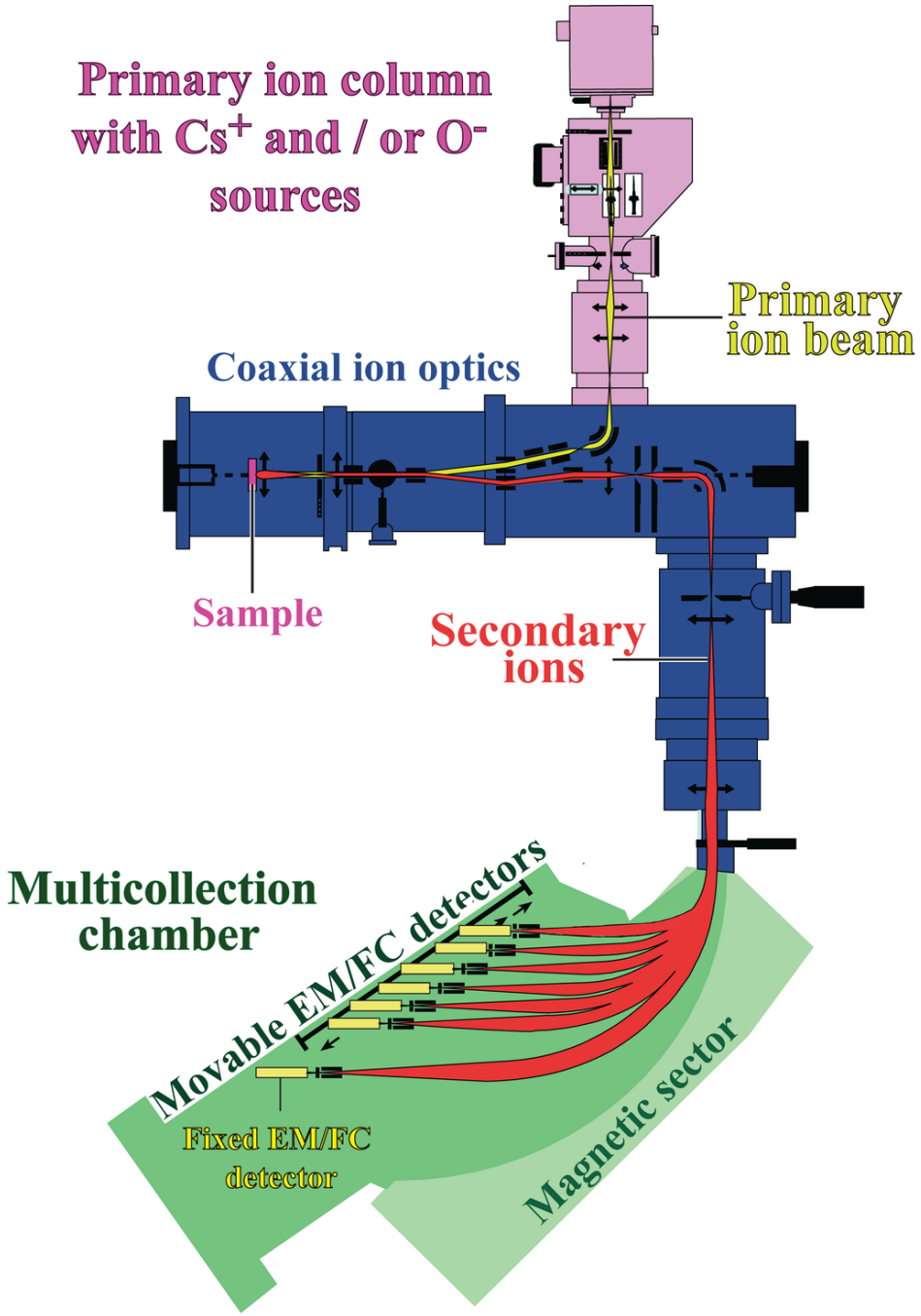

Figure 11. Illustration of the NanoSIMS 50L instrument. A cesium or oxygen primary ion source generates a focused primary ion beam that scans the sample surface. Emitted secondary ion species are separated in the dual-focusing mass analyzer and detected in parallel with 5 (NanoSIMS 50) or 7 (NanoSIMS 50L) detectors in the multicollection chamber. The lateral resolution is improved by reduction of the primary ion beam spot size with the co-axial ion optics. EM-Electron multiplier; FC-Faraday cup. Scheme is adapted with permission from reference [112] and modified by the author of the thesis.

environmental microbiology,[160] and cell biology.[161] In a comparison to other SIMS techniques, the superior spatial resolution capability of magnetic sector SIMS has allowed it to be applied in biological studies, especially for imaging cells and sub-cellular compartments.[162] In such studies, a 16 keV energy Cs^+ primary ion beam is commonly applied. Stable isotopes such as ^2H, ^{13}C, ^{15}N, and ^{18}O are used to label target molecules. Owing to the excellent mass resolution with high transmission, the NanoSIMS is capable of resolving ion species such as $^{13}C^{12}C^-$ and $^{12}C_2^-$ and even isobars with same nominal mass like $^{12}C^{15}N^-$ and $^{12}C^{14}N^1H^-$.

As with the ToF-SIMS instrument, the NanoSIMS operates in an ultra-high vacuum environment and thus water rich samples necessitate adequate preparation. Preservation of biological specimens requires attention as soluble compounds can migrate or even be completely lost during sample preparation. Several conservation strategies have been proposed. Some of them are common fixation protocols employed in the electron microscopy field, such as chemical fixation and cryo-fixation with freeze substitution (FS), as described in Chapter 3. Hence, chemical processing of the sample with chemical fixation has been proposed for immobilization of non-diffusible chemical species or species that can form chemical bonds with the fixatives and therefore become entrapped. Cryo-fixation with FS is a suitable approach if the analytes of interest are the chemical species that are prone to diffuse.[120,163,164] If the nature of the sample does not allow application of typical electron microscopy sample preparation protocols, for example when imaging of lipids, one might consider freeze-drying as a solution. This involves plunge-freezing of the specimen and consequently slow drying at low temperature to allow removal of vitreous ice.[124,165,166]

Combining the NanoSIMS with other imaging techniques enables obtaining a chemical and the structural information needed to understand biological processes. Hence, Takado et al. performed a set of experiments to investigate glycogen metabolism in liver and brain tissues by administrating ^{13}C-labeled glucose into the mice. The correlation of NanoSIMS imaging data with TEM micrographs (Fig. 12), both obtained from the same specimen area, revealed the subcellular localization of the target molecules with chemical information. This allowed precise subcellular localization of glucosyl residues and their quantification as the $^{13}C/^{12}C$ isotopic ratio at the nanometer scale.[167]

NanoSIMS has the capability to image proteins by pulsing isotopically labeled amino acids[168] into the cell. However, understanding metabolism at the subcellular level, and the study

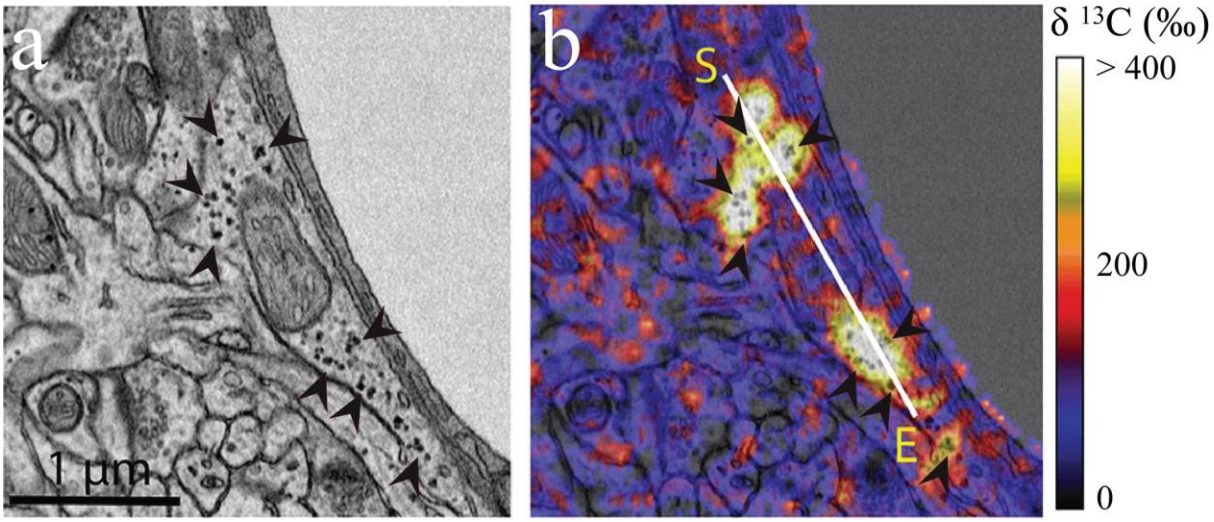

Figure 12. NanoSIMS correlation with a TEM technique. (**a)** TEM image of brain section (arrows in black indicate glycogen granules); (**b**) Chemical map showing ^{13}C enrichment of the same area in TEM image. The ^{13}C enrichment is expressed in the delta notation: $\delta\ ^{13}C\ (‰) = (\frac{Cmes}{Cnat} - 1)\ x\ 1000$, where C_{mes} is measured $^{13}C/^{12}C$ ratio, C_{nat} is the mean of natural $^{13}C/^{12}C$ ratio. The incorporation of the uniformly labelled ^{13}C glucose contributes to a far higher ‰ of ^{13}C in the regions containing the glycogen. Adapted with permission from the reference.[167]

of protein complexes is still limited as NanoSIMS cannot provide chemical information of specific proteins.[161,168] Attempt to improve the specificity of protein imaging have been carried out.[169] Here, NanoSIMS was used for imaging cells labeled with metals, such as lanthanides conjugated antibodies. The chemical distribution of the different lanthanide elements corresponded to a specific antibody and therefore to a specific epitope. Although this methodology allows single-step specific protein analysis, without the need to correlate with other imaging technique(s), it suffers from a difficulty in targeting some epitopes with antibodies.[169] Moreover, metal labeled antibodies react only with a small portion of the epitopes, and therefore their incorporation into the biological sample is rather poor.[170] This can degrade the high-spatial resolution of NanoSIMS and therefore less-precise images will be acquired.

In order to make a step forward in identifying specific organelles and proteins, a methodology where stimulated emission depletion (STED) microscopy and NanoSIMS are correlated has been developed (Fig. 13a). This nanoscopic approach has allowed the investigation of the turnover of different cellular structures such as membranes, organelles, and protein clusters. The correlation approach to combine STED and NanoSIMS has been named correlated optical isotopic nanoscopy (COIN).[168] Although COIN is a very powerful approach, there are some

restrictions to this methodology such as the necessity to use two very expensive instruments, the difficulty to get some antibodies to incorporate into the specimen, and to find a sufficient number of epitopes in order to obtain accurate nanoscopic imaging. Recently, an elegant approach for specific isotopic and fluorescent protein labeling has been developed with genetic-code expansion followed by chemoselective click-chemistry labeling (Fig. 13b).[171]

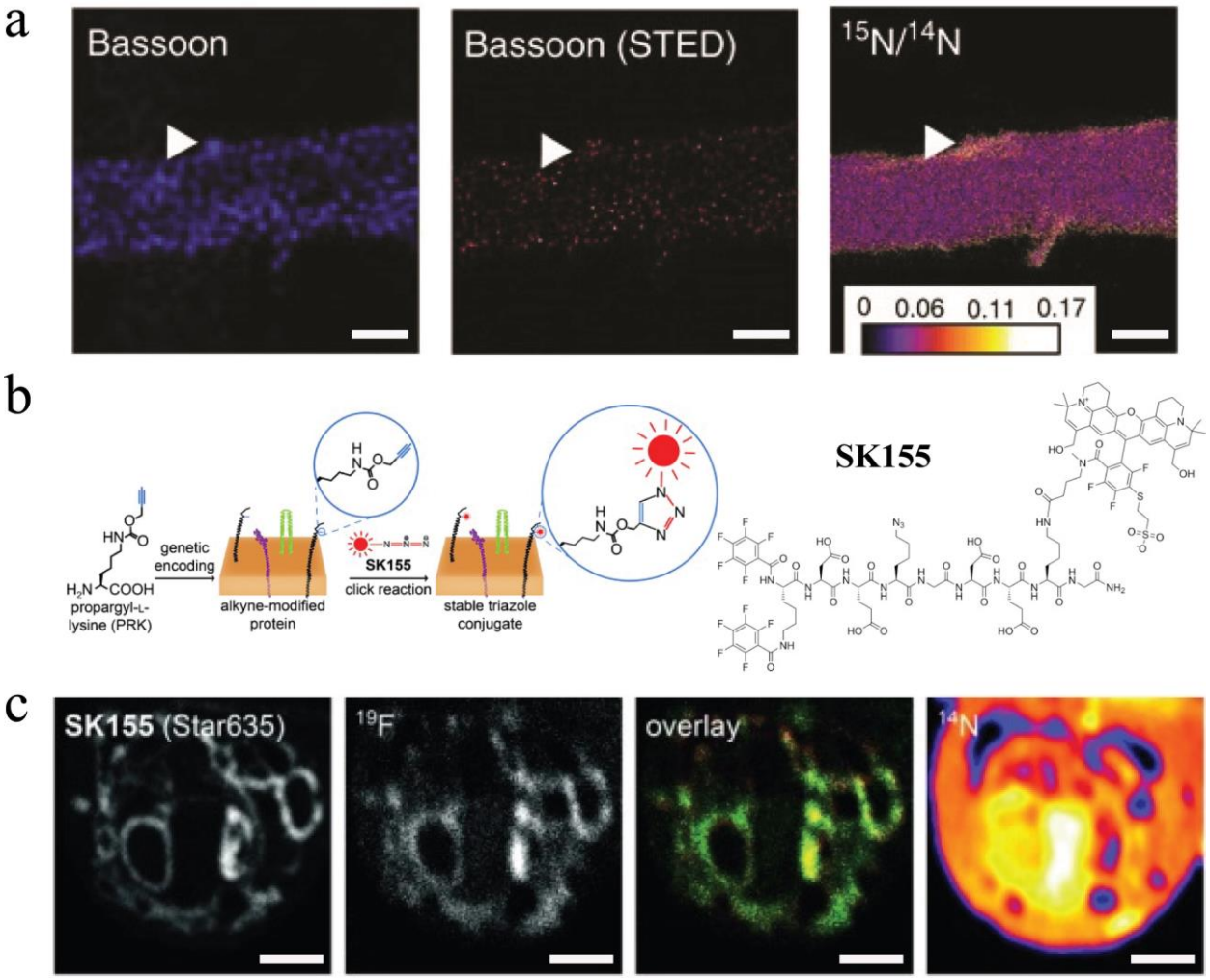

Figure 13. Correlated optical isotopic nanoscopy (COIN). (**a**) Immunocytochemically and isotopically labeled proteins in the neuronal axon. From left to right: Confocal image, bassoon (active zone marker); STED image of bassoon; NanoSIMS image of ^{15}N-enrichment. The elevated $^{12}C^{15}N^-/^{12}C^{14}N^-$ ratio has been assigned to a synapse via confocal and STED images and is indicated with an arrow. Scale bar: 2 µm. (**b**) Schematic representation of genetic-code expansion via unnatural amino acids (UAA). UAA was introduced into the protein of interest and labeled via click reaction with the probe SK155, which can be used in both, fluorescence and NanoSIMS imaging; (**c**) Imaging data for genetically-encoded protein syntaxin in fibroblasts. From left to right: Confocal image of Star635; NanoSIMS ion image of $^{19}F^-$; Overlay of Star635 signal (red) and $^{19}F^-$ (green); NanoSIMS ion image of $^{12}C^{14}N^-$ ion species revealing cellular features. Scale bar: 2 µm. Adapted with permission from the references.[168,171]

This labeling approach enables the application of an unnatural amino acid (UAA), which can be incorporated into the protein of interest. Its DNA was modified to harbor an Amber STOP codon, that determines the binding site for the UAA and pair of tRNA and aminoacyl-tRNA synthetase to introduce the UAA into the specific protein. The UAA is revealed after cellular fixation when a custom synthesized probe is introduced containing fluorophore and isotopes (Fig. 13c). Even though the fluorophore is not particularly necessary in these experiments, it is useful to test the probe with fluorescence microscopy.[171]

4.2. Electrochemistry

Electrochemical techniques offer versatile tools to study neurochemistry as some key neurochemicals, like the biogenic amines, are easily oxidized.[172,173] Frequently employed electrochemical techniques that are used to monitor, detect and measure the concentration or quantify various electroactive neurochemical species *in vivo* as well as *in vitro* are fast scan cyclic voltammetry (FSCV) and amperometry.[174,175] FSCV provides chemical specificity and reduces the possibility that the data will be interpreted wrongly in the presence of interferents.[176,177] For this reason, FSCV has become a convenient tool to study some complex systems in the brain.[178] However, its temporal resolution is rather poor relative to the fast exocytosis events that typically occur in milliseconds. Thus, the faster amperometry electrochemical technique has been adapted for exocytosis studies.[175,178,179] Amperometry also offers quantification of the numbers of molecules released during exocytosis events.

4.2.1. Single cell amperometry

Since development of the carbon fiber disk microelectrodes,[180,181] and their later use to monitor individual exocytotic events at chromaffin cells,[173,182] the era of *single cell amperometry* (SCA) begun. SCA was applied to measure the transmitter release from a variety of cell types such as mast cells, pancreatic beta-cells,[183] PC12 cells,[184] and neurons.[185,186] Its application in revealing the exocytosis mechanistic details as well as gaining the new insights into behaviour of SSVs and LDCVs are still in progress.

Since single cell amperometry exhibits currents in the nano- and even picoampere range and demands high spatial resolution, application of *carbon-fiber microelectrodes* that demonstrate high sensitivity, low levels of noise, and have small size, is very useful. In addition to this, they are characterized by biocompatibility, inexpensiveness, flexibility, and relatively easy to manufacture.

Generally, in a SCA setup, a disk carbon fiber microelectrode is placed on a top of the cell and held at a constant potential (usually <1.0 V vs. a Ag|AgCl reference electrode), which oxidizes the analyte of interest. The cell undergoes exocytosis following exposure to electrical stimulation or a chemical secretagogue such as elevated concentration of potassium ions. As the vesicles fuse with the plasma membrane, they release neuromessenger that is oxidized at the carbon fiber surface

releasing electrons detected as current (Fig. 14). The electrons generate current spikes in an amperometric trace.

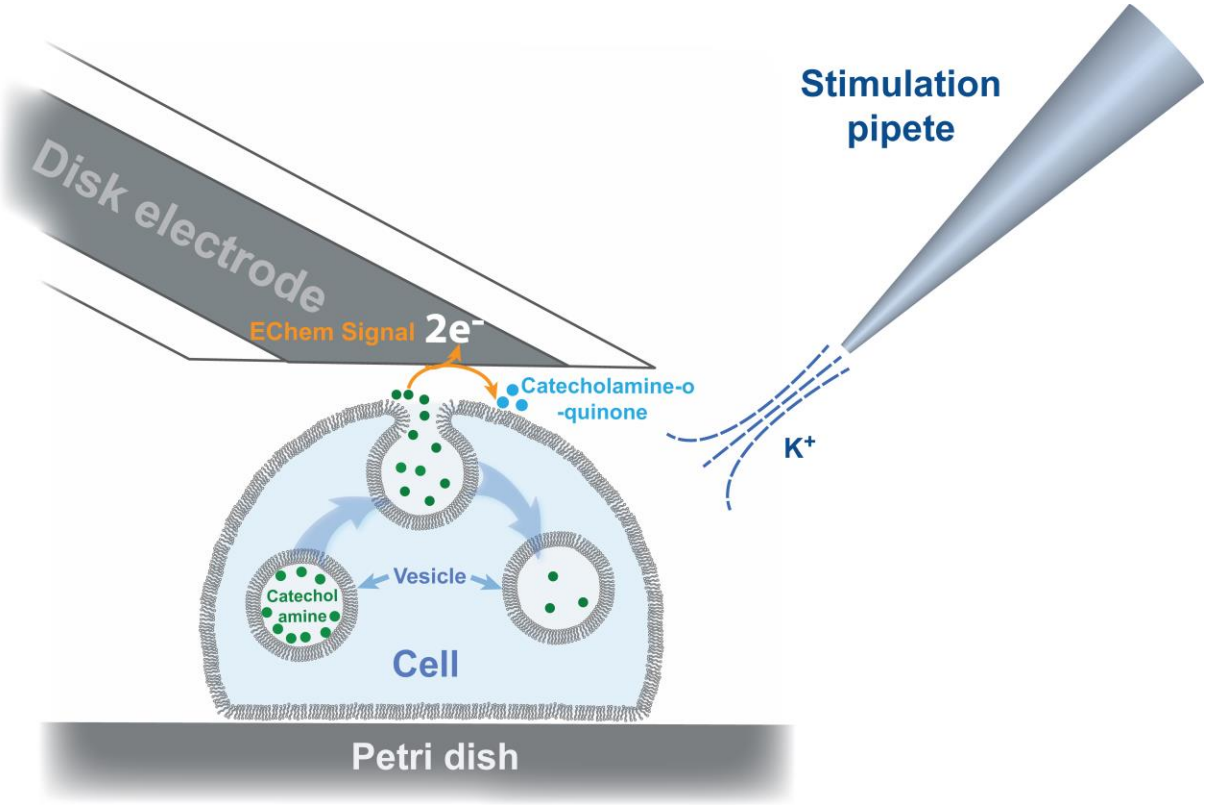

Figure 14. Single cell amperometry setup for measuring the release of neurotransmitters at a disk carbon-fiber microelectrode during stimulated exocytosis. A microelectrode is placed onto the cell and the exocytosis is triggered by K^+ ions at elevated concentration. By holding the microelectrode sensor at a constant potential (typically 700 mV vs. a Ag|AgCl reference electrode), the neurotransmitters are oxidized releasing electrons (2 e^- for each catecholamine molecule) that can be measured as current transients (see Fig. 15).

The amperometric spikes give valuable information about exocytotic events. The amount of transmitters released, *N*, can be calculated by using *Faraday's law* (Fig. 15), from the charge, *Q*, measured, the number of electrons, *n*, that are exchanged in the oxidation reaction (2 e^- for each oxidized catecholamine molecule), and Faraday's constant, *F* (96,485 $Cmol^{-1}$). Moreover, the shape of the amperometric peak provides information about the kinetics of transmitter release (Fig 15). Accordingly, the peak current amplitude (I_{max}) defines the maximum flux of released analyte, the duration of the event is summarized by the half-width of the peak ($t_{1/2}$), the rise time (t_{rise}) is related to the time that it takes for a fusion pore to open, and the fall time (t_{fall}) is that needed for the oxidation of the secretory vesicle content or the vesicle to close again.[187-189]

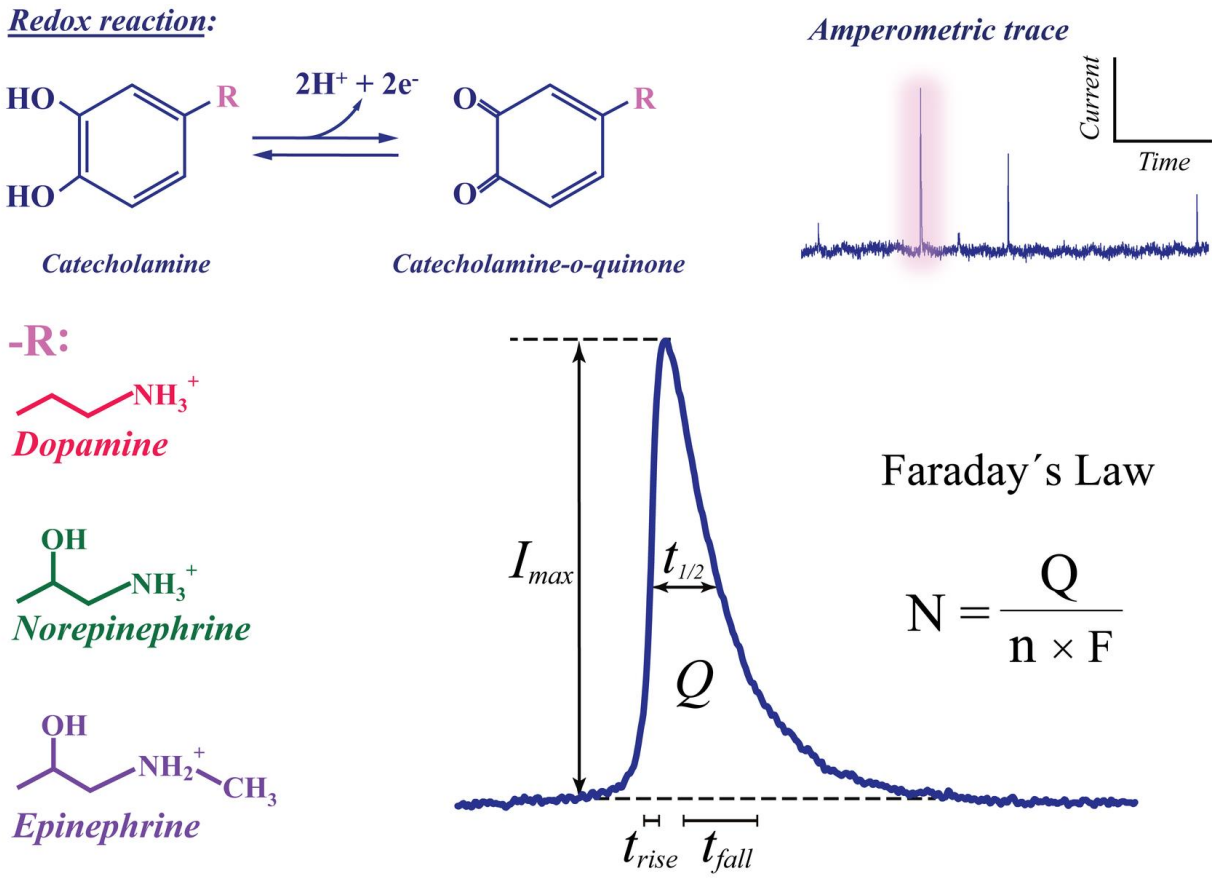

Figure 15. Amperometric measurement of oxidizable catecholamine release provides quantitative and kinetic information about exocytotic events. An enlarged current spike from a typical amperometric trace shows how the quantitative data is obtained by employing Faraday's law. It shows additionally the kinetic parameters of the release events (I_{max}, t_{rise}, t_{fall}). *N*, the amount of transmitter released; *Q*, charge; *n*, number of electrons transferred in the oxidation reaction; *F*, Faraday's constant (96,485 $Cmol^{-1}$). Kinetic peak parameters: I_{max}, maximum flux of the released analyte; $t_{1/2}$, width of the peak at half maximum; t_{rise}, time from 25% to 75% of the front side of each peak; t_{fall}, time from 75% to 25% of the backside of each current transient.

In this thesis, SCA was employed to measure and quantify the neurotransmitters released during exocytosis from stimulated PC12 cells that have been pharmacologically manipulated and the data was correlated with the results obtained from NanoSIMS imaging. The study is presented in the **Paper V** of the thesis.

4.2.2. Vesicle electrochemical cytometry

Although single cell amperometry provides valuable insights into the transmitter quanta during exocytotic release, it still suffers from an inability to quantify the entire content of a vesicle. In order to gain direct evidence that the exocytosis process involves partial release, several methodologies have been developed to measure the total neurotransmitter cargo present in the secretory vesicles. The first methodological approach for this quest was developed by Omiatek et al. and was called *electrochemical cytometry*.[190] It uses a microfluidic-based platform to separate and lyse individual transmitter filled liposomes or secretory vesicles that have been isolated from cells or tissues and quantify their electroactive content. The separation and detection of soft nanoparticles has been achieved with capillary electrophoresis and end-column electrochemical detection, respectively. This methodology was first tested by measuring the catecholamine content of filled unilamellar liposomes[190] and was followed with studies to quantify the neurotransmitter content present in vesicles isolated from PC12 cells[60] or mouse brain tissue.[191]

More recently, several research groups have reported a technology based on the same principle but without the separation step to probe the content of single nanoparticles. Hence, different soft nanoparticles have been probed, such as emulsion droplets,[192] liposomes[193] and the secretory vesicles.[194] In the last case, the study is presented in **Paper I** of the thesis and this methodology has been called *vesicle electrochemical cytometry*. Here, a disk carbon-fiber microelectrode is placed into a suspension of LDCVs, isolated from bovine adrenal medulla, that adsorb onto the electrode surface and rupture releasing their oxidizable content (Fig. 16).[194]

Vesicle electrochemical cytometry was also applied in the study described in **Paper II**. Here, I studied dopamine filled liposomes and compared the response to vesicles and liposomes with added peptides to mimic the native transmitter vesicles. These were probed in order to gain understanding of the rupture mechanism of soft nanoparticles as they open onto the carbon fiber electrode surface.[195]

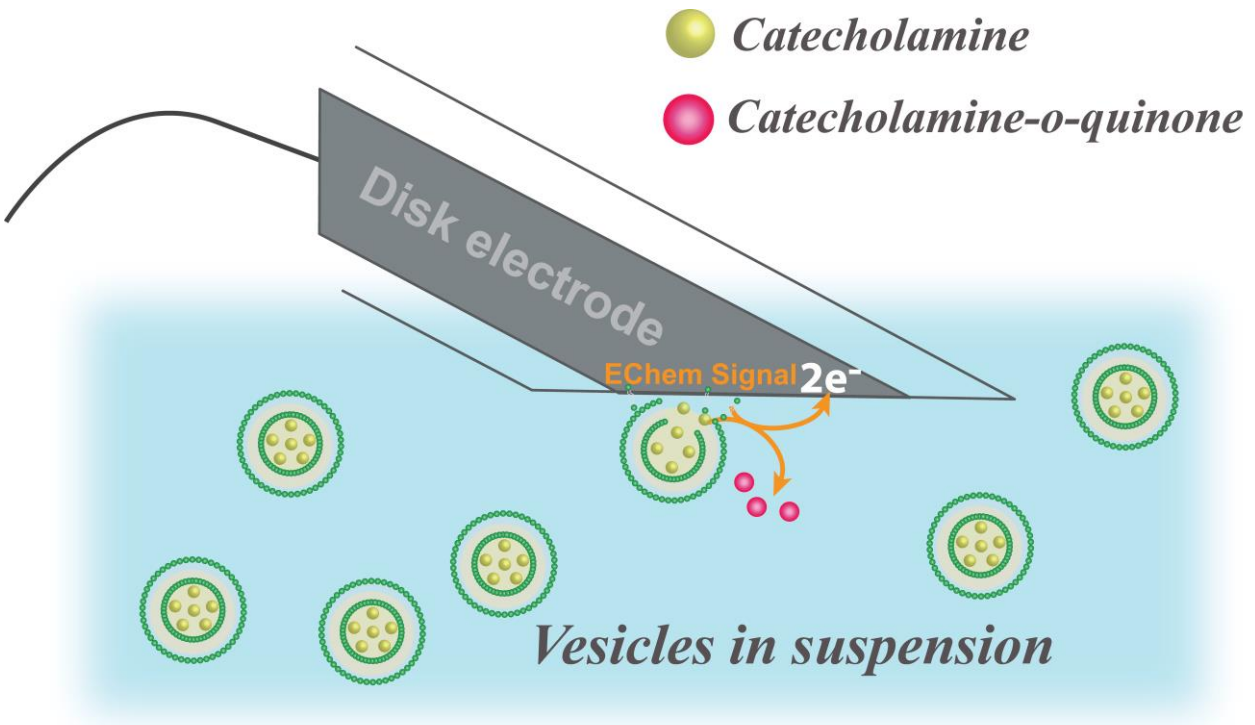

Figure 16. Schematic representation of vesicle electrochemical cytometry. A 33-μm diameter disk carbon-fiber microelectrode is submerged into the suspension of transmitter liposomes or native vesicles isolated from neuroendocrine cells. By applying a constant potential (ca. +700 mV vs. a Ag|AgCl reference electrode) at the carbon-fiber microelectrode, the current transients are recorded when the liposomes or native vesicles that are in the contact with the sensor, open the pore that is formed at the membrane-electrode junction and expose oxidizable cargo.

Most recently, a method to probe secretory vesicle content inside living cells has been developed. Here, the vesicle transmitters are quantified directly in the cell cytoplasm, therefore there is no more demand for the vesicle isolation. More importantly, it allows direct and real-time pharmacology to be applied and it allows direct comparison of the vesicular amount and the amount released during exocytosis. This approach is called *intracellular vesicle electrochemical cytometry*[61] and its principle is shown in Figure 17.

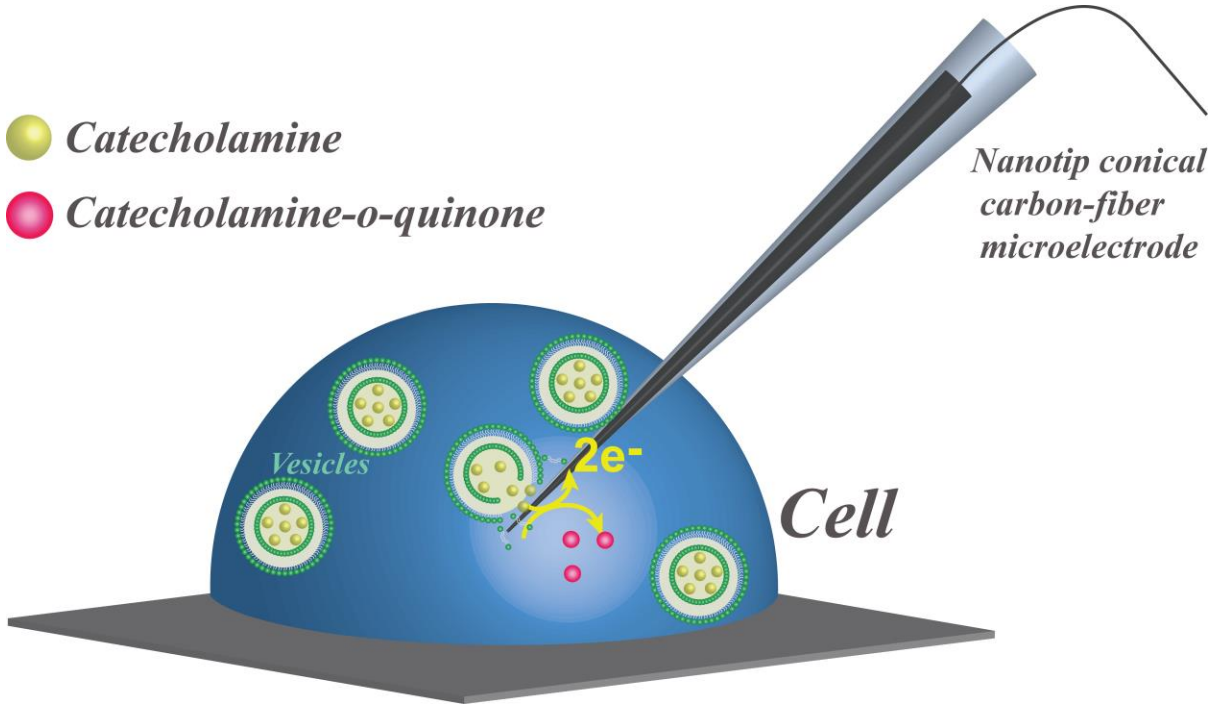

Figure 17. Schematic representation of intracellular vesicle electrochemical cytometry. A nanotip conical carbon-fiber microelectrode is inserted into the cytoplasm of the single cell and held at the constant potential (ca. +700 mV vs. a Ag|AgCl reference electrode). The conical tip of the electrode is exposed to the catecholamine containing vesicles. The vesicles adsorb at the sensor surface and later rupture releasing their electroactive content that can be amperometrically measured.

Here, Li et al. employed a flame-etched nanotip conical carbon-fiber microelectrode[196] that was gently inserted into the PC12 cell cytoplasm without significantly damaging the plasma membrane. Thus, the electrode surface was exposed to the vesicles containing electroactive dopamine and its amount was measured *in situ* while the cell was still alive. Due to vesicle adsorption and subsequent rupture at the electrode, the dopamine content was determined by applying constant potential (ca. +700 mV vs. a Ag|AgCl reference electrode) at the electrode. In **Paper V** intracellular vesicle electrochemical cytometry was used to complement the NanoSIMS measurements and to quantify the neurotransmitter content in PC12 cell vesicles that have been pharmacologically manipulated with L-DOPA and reserpine.

5 SUMMARY OF PAPERS

The main aim of this thesis has been to probe the total content of the dense core secretory vesicles and their artificial mimics, the liposome model systems, by utilizing analytical tools like electrochemistry and secondary ion mass spectrometry imaging. Hence, the experiments, even though having the same essential goal can be divided into two units. In the first part, **Papers I** and **II**, amperometry was employed to analyze the transmitter content of chromaffin secretory vesicles and their analogues, liposomes. In the second part, **Papers III**, **IV** and **V**, the methodologies to image the vesicle and liposome contents have been developed and performed with two high-resolution imaging techniques, ToF-SIMS and NanoSIMS.

In **Paper I**, a new approach called vesicle electrochemical cytometry (VEC) has been developed to characterize in a collision-adsorption manner, the content of individual nanometer-size chromaffin secretory granules. This has proven to be a robust and simple methodology to analyze the electroactive catecholamine content of single vesicles. In VEC, a 33-μm diameter disk-shaped carbon electrode has been employed and immersed in a suspension of isolated adrenal medullary vesicles. The transmitter content is trapped against the electrode surface when the secretory vesicles adsorb and open at the carbon-fiber microelectrode. The transmitter is then oxidized and the recorded amperometric current transients correspond to single vesicle bursting events. A large number of amperometric spikes (86%) were associated with single vesicle ruptures that can be picked out from the data, allowing accurate quantification of the vesicular catecholamine content.

To understand the mechanism of the vesicle rupture process in electrochemical vesicle cytometry, a study was carried out in **Paper II** in order to measure and model the vesicle bursting events at mimic systems. The data suggest that electroporation plays an important role in a formation of the pore between the vesicle membrane and the electrode surface. This phenomenon restricts the content from diffusing away and thus allows quantitative oxidization. Investigation of the influence of native membrane proteins on rupture dynamics was considered. When lipid-only transmitter-loaded liposomes were used they showed faster rupture events in comparison with native vesicles. More complex liposome systems were synthesized by decorating the surface of the liposome with surface peptide to mimic the protein component of the native membrane. Interestingly, the kinetics of bursting for the peptide-decorated particles was between that of liposomes and native vesicles. This suggests that electroporation occurs after the membrane

proteins migrate away from the interface thus allowing a tighter contact between the membrane and the electrode. Additionally, the models presented suggest that the protein dense core in chromaffin vesicles used here decreases the dynamics of the events by reducing the catecholamine diffusion through the vesicle interior.

In **Paper III** the chemistry of native vesicle models such as micrometer size liposomes was investigated by ToF-SIMS imaging and depth profiling. Two models of giant liposomes were analysed, histamine-containing liposomes resembling the clear vesicles, and ATPS-containing liposomes that mimic the LDCVs. Mass spectrometric imaging and depth profiling were done with only the C_{60}^{+} beam and in the dual beam mode using C_{60}^{3+} for etching and Bi_3^{+} for analysis. In this work it has been shown that ToF-SIMS has the potential with two-dimensional imaging and depth profiling to reveal the inner morphology of liposomes, showing their micro-compartmentalization.

The correlation between two high-spatial resolution imaging techniques, ToF-SIMS and NanoSIMS, is shown in **Paper IV**. Here, ToF-SIMS was applied as a tool to screen the chemistry in chemically fixed adrenal cells prepared for TEM imaging. Numerous specific ion species originating from osmium tetroxide that was used as a fixative and stain were detected and localized in lysosomes, specific subcellular compartments of the adrenal cells. This allowed preselection of the ion specie $^{190}Os^{16}O^{-}$ for a subsequent NanoSIMS imaging experiment and it revealed that it localizes in the lysosomes as detected by ToF-SIMS. Results published in Paper IV demonstrate the capability of ToF-SIMS to be a screening tool in optimization of NanoSIMS high-resolution imaging, and in the future might replace TEM for localization of subcellular features.

In **Paper V**, the vesicle storage mechanism has been investigated by pharmacologically manipulating the LDCVs in PC12 cells with L-DOPA and reserpine administration. The methodology to look into and spatially resolve the chemistry of isotopically labeled dopamine across single secretory vesicles by employing high-resolution mass spectrometry imaging, NanoSIMS, has been established. Furthermore, combining NanoSIMS with novel electrochemical techniques provided a means to quantify the vesicle content and compare to the NanoSIMS relative quantification. This study revealed that dopamine relocation between vesicular compartments, the dense core and the halo, is kinetically limited. It appears that vesicle inner morphology has an important role in regulation of the neurotransmitter kinetics inside the secretory vesicles. Lastly, by combining TEM with NanoSIMS imaging, impressive images have been obtained showing the dopamine profiles across the single nanometer-size vesicles.

6 CONCLUDING REMARKS AND OUTLOOK

The work presented in this thesis focused on the aim of developing the methodological solutions for analyzing the total content of secretory vesicles of neuroendocrine cells and models. The motivation for this research sprang out from the need to understand the mechanism of exocytosis and to attempt to discover evidence for the partial release mechanism of large dense core vesicles present in endocrine cells and neurons as well. This is not a simple task since nanometer-size vesicles contain less than 10^{-18} moles of neurotransmitter. Therefore, a need emerged to establish new bioanalytical methodologies that would be sensitive enough and have high spatial and temporal resolution to detect minute amounts of vesicular transmitters and could provide snapshots of the nanometer-size secretory vesicles and their cargo. Therefore, in this thesis, two nano-scale analytical tools, electrochemistry and imaging mass spectrometry are used to address these essential questions.

The methodology to electrochemically probe the single vesicle transmitter load, called electrochemical cytometry, was developed in 2009 by the Ewing group. However, in this thesis VEC was demonstrated to be a simpler approach. For more than eighty percent of all events, only single vesicles open on the electrode surface, showing that VEC is an effective technique to quantify the epinephrine and norepinephrine amounts in chromaffin vesicles. This technique with its high sensitivity and spatio-temporal resolution has the potential for furthering understanding of different phenomena that were shown in a Paper II where dopamine containing liposome model systems were used to reveal the rupture mechanism of the native vesicles. Even more, it was demonstrated that the polarized electrode surface has a significant effect on the vesicle rupturing by means of electroporation. VEC offers the opportunity to probe the content of other vesicular systems, maybe to alter the lipid membrane composition of the liposomes or even to introduce more complex membrane components such as enzymes and correlate the membrane properties to the kinetics of the rupturing events.

Beside electrochemistry, secondary ion mass spectrometry imaging has been shown to have high potential for probing the structure and content of secretory vesicles and liposome systems. The first study in this thesis employed ToF-SIMS, which has been used to surface analyze and depth profile a micrometer-size liposome system that was used to mimic native vesicles. It was shown that ToF-SIMS can detect the micro-compartmentalization phenomenon in frozen-hydrated ATPS liposomes and, additionally, with its high-mass resolution capability clearly resolve the

signal of the classical transmitter, histamine in a mass spectrum. The spatial resolution of the ToF-SIMS is still not sufficient for analyzing smaller sub-cellular features such as the vesicles of chromaffin cells and neurons. However, it offers the possibility to study other biological systems in the frozen-hydrated state, thus preserving the chemistry and inner morphology of the analyzed sample. An interesting ToF-SIMS application in the future would be to study the histamine distribution across the LDCVs of mast cells present in the mutant beige mouse where the secretory vesicles are as large as 4 μm in diameter. These would be large enough to spatially resolve with this imaging technique.

In order to analyze smaller secretory vesicles, high-resolution SIMS, NanoSIMS has been recruited to probe dopamine content inside the LDCVs of the PC12 cell line. This was successfully performed by isotopically labeling dopamine molecules for detection, and preserving their native location by the means of chemical fixation. Pharmacological cell treatments with the dopamine precursor, L-DOPA, and the VMAT inhibitor, reserpine, allowed manipulation of the vesicle transmitter storage and furthermore it revealed a kinetic limitation for dopamine distribution between the vesicular compartments, the dense core and the halo. In order to make the NanoSIMS analysis easier, PC12 cell sections were imaged by TEM to locate LDCVs and their inner compartments for the subsequent NanoSIMS imaging. This step absolutely improved the experiment. Yet, in Paper IV, I showed that ToF-SIMS, used as a screening tool, is capable of distinguishing different osmium oxide ion species in the lysosomes of adrenal cells and this was confirmed by the NanoSIMS later in the same study. Since the dense cores in LDCVs are massively enriched in osmium tetroxide when fixed this way, they manifest as a dark color under the electron beam in the TEM. It would be very interesting to look for the osmium oxide ion species in LDCVs by NanoSIMS. This would implicate that the osmium oxide signal correlates with the dense core. This approach would perhaps make it possible to avoid previous TEM imaging and allow direct correlation between dopamine and osmium oxide ion maps and more conclusive observations about dopamine distribution between subvesicular compartments. If we can find other markers in the ToF-SIMS, we might avoid the osmium fixation overall by avoiding the TEM and correlating images between static and dynamic SIMS, if the future spatial resolution of ToF-SIMS will allow that.

In conclusion, the data and the methods presented in this thesis have great potential to expand the knowledge related to the storage mechanism of the secretory vesicles and to further the understanding of the exocytosis process in general.

7 ACKNOWLEDGEMENTS

I would genuinely like to thank following people for contributing during my doctoral studies:

First of all, I would like to thank my supervisor **Andrew Ewing** for seeing the potential in me for scientific research and giving the opportunity to do doctoral studies. Thank you for all your support especially for teaching me how to be creative, constructive, focused and practical. I would particularly like to thank you for motivating me to be persistent especially during my PhD moments when I was 'stuck in a rut'. I really appreciate it.

My second supervisor **John Fletcher** for always being positive and excited about the science. Thank you for the all great mass spec discussions.

My excellent lab buddy, **Neda** for great times together, a lot of laughter and fun night shifts! Thank you for being always supportive, reliable and trying to learn Serbian! You have a perfect accent! Zdravo, kako si? ☺

To **Mike**, for being always creative when needed and teaching me how to improve scientific writing. ☺ Thank you for making me laugh in crisis moments and for all fun times in the NanoSIMS cave. And for the fancy coffees!

My colleague, **Per** for great mass spec discussions and support on my PhD road. Thank you for always being ready to meet and answer the e-mails ASAP. ☺

All the past and present members of the **Ewing**, **Fletcher**, **Cans**, **Hanrieder** and **Safina** research groups. Thank you for all the discussions in group meetings and social activities.

The **members** of the Electron Microscopy Unit at Sahlgrenska Academy for the nice EM discussions and fun times.

All the **co-authors** of the manuscripts for productive collaboration and great discussions.

All **colleagues** from 4th floor and from Division of Chemistry and Biochemistry for nice lunch-coffee breaks and pleasant working environment.

My friends, for all your support and always being there in times needed.

Мојој породици, за вашу безусловну љубав и подршку.

8 REFERENCES

[1] Kandel, E. R., **Principles of Neural Science.** McGraw-Hill Medical: 2013.

[2] Alberts, B., **Molecular biology of the cell.** Garland Publ: New York, 1983.

[3] Katz, B.; Miledi, R., **Spontaneous and evoked activity of motor nerve endings in calcium Ringer.** *The Journal of Physiology* 1969**,** *203* (3), 689-706.

[4] Meldolesi, J.; Ceccarelli, B., **Exocytosis and Membrane Recycling.** *Philosophical Transactions of the Royal Society of London B: Biological Sciences* 1981**,** *296* (1080), 55-65.

[5] Kelly, R. B., **Storage and release of neurotransmitters.** *Cell* 1993**,** *72 Suppl*, 43-53.

[6] Südhof, T. C., **The synaptic vesicle cycle: a cascade of protein-protein interactions.** *Nature* 1995**,** *375* (6533), 645-653.

[7] Burgoyne, R. D.; Morgan, A., **Analysis of regulated exocytosis in adrenal chromaffin cells: insights into NSF/SNAP/SNARE function.** *Bioessays* 1998, *20* (4), 328-35.

[8] Edwards, R. H., **The neurotransmitter cycle and quantal size.** *Neuron* 2007, *55* (6), 835-58.

[9] Pereira, D. B.; Sulzer, D., **Mechanisms of dopamine quantal size regulation.** *Front. Biosci. (Landmark Ed)* 2012, *17*, 2740-67.

[10] Palfrey, H. C.; Artalejo, C. R., **Vesicle recycling revisited: rapid endocytosis may be the first step.** *Neuroscience* 1998, *83* (4), 969-89.

[11] de Toledo, G. A.; Fernandez-Chacon, R.; Fernandez, J. M., **Release of secretory products during transient vesicle fusion.** *Nature* 1993, *363* (6429), 554-558.

[12] Staal, R. G. W.; Mosharov, E. V.; Sulzer, D., **Dopamine neurons release transmitter via a flickering fusion pore.** *Nat. Neurosci.* 2004, *7* (4), 341-346.

[13] Wightman, R. M.; Haynes, C. L., **Synaptic vesicles really do kiss and run.** *Nat. Neurosci.* 2004, *7* (4), 321-322.

[14] Aravanis, A. M.; Pyle, J. L.; Harata, N. C.; Tsien, R. W., **Imaging single synaptic vesicles undergoing repeated fusion events: kissing, running, and kissing again.** *Neuropharmacology* 2003, *45* (6), 797-813.

[15] Ales, E.; Tabares, L.; Poyato, J. M.; Valero, V.; Lindau, M.; Alvarez de, T., **High calcium concentrations shift the mode of exocytosis to the kiss-and-run mechanism.** *Nat. Cell. Biol.* 1999, *1* (1), 40-44.

[16] Ren, L.; Mellander, L. J.; Keighron, J.; Cans, A.-S.; Kurczy, M. E.; Svir, I.; Oleinick, A.; Amatore, C.; Ewing, A. G., **The evidence for open and closed exocytosis as the primary release mechanism.** *Quarterly Reviews of Biophysics* 2016, *49*, e12 (27 pages).

[17] Artalejo, C. R.; Elhamdani, A.; Palfrey, H. C., **Secretion: Dense-core vesicles can kiss-and-run too.** *Current Biology* 1998, *8* (2), R62-R65.

[18] Amatore, C.; Bouret, Y.; Travis, E. R.; Wightman, R. M., **Interplay between membrane dynamics, diffusion and swelling pressure governs individual vesicular exocytotic events during release of adrenaline by chromaffin cells.** *Biochimie* 2000, *82* (5), 481-496.

[19] Mellander, L. J.; Trouillon, R.; Svensson, M. I.; Ewing, A. G., **Amperometric post spike feet reveal most exocytosis is via extended kiss-and-run fusion.** *Scientific Reports* 2012, *2*, 907.

[20] Park, Y.; Kim, K.-T., **Short-term plasticity of small synaptic vesicle (SSV) and large dense-core vesicle (LDCV) exocytosis.** *Cellular Signalling* 2009, *21* (10), 1465-1470.

[21] Yao, J.; Erickson, J. D.; Hersh, L. B., **Protein Kinase A Affects Trafficking of the Vesicular Monoamine Transporters in PC12 Cells.** *Traffic* 2004, *5* (12), 1006-1016.

[22] Plattner, H.; Artalejo, A. R.; Neher, E., **Ultrastructural organization of bovine chromaffin cell cortex-analysis by cryofixation and morphometry of aspects pertinent to exocytosis.** *J. Cell. Biol.* 1997, *139* (7), 1709-17.

[23] Bauerfeind, R.; Huttner, W. B., **Biogenesis of constitutive secretory vesicles, secretory granules and synaptic vesicles.** *Curr. Opin. Cell. Biol.* 1993, *5* (4), 628-35.

[24] Patzak, A.; Winkler, H., **Exocytotic exposure and recycling of membrane antigens of chromaffin granules: ultrastructural evaluation after immunolabeling.** *J. Cell. Biol.* 1986, *102* (2), 510-5.

[25] Colliver, T. L.; Pyott, S. J.; Achalabun, M.; Ewing, A. G., **VMAT-Mediated changes in quantal size and vesicular volume.** *Journal of Neuroscience* 2000, *20* (14), 5276-5282.

[26] Robberecht, P.; Lingier, P.; Woussen-Colle, M. C., **Current status on chromogranin A and pancreastatin.** *Acta Gastroenterol. Belg.* 1993, *56* (3-4), 261-3.

[27] Johnson, R. G., **Accumulation of biological amines into chromaffin granules: a model for hormone and neurotransmitter transport.** *Physiological Reviews* 1988, *68* (1), 232-307.

[28] Banks, P.; Helle, K., **The release of protein from the stimulated adrenal medulla.** *Biochemical Journal* 1965, *97* (3), 40C-41C.

[29] Taupenot , L.; Harper , K. L.; O'Connor , D. T., **The Chromogranin–Secretogranin Family.** *New England Journal of Medicine* 2003, *348* (12), 1134-1149.

[30] Montero-Hadjadje, M.; Elias, S.; Chevalier, L.; Benard, M.; Tanguy, Y.; Turquier, V.; Galas, L.; Yon, L.; Malagon, M. M.; Driouich, A.; Gasman, S.; Anouar, Y., **Chromogranin A Promotes Peptide Hormone Sorting to Mobile Granules in Constitutively and Regulated Secreting Cells: Role of conserved n- and c-terminal peptides.** *Journal of Biological Chemistry* 2009, *284* (18), 12420-12431.

[31] Winkler, H.; Westhead, E., **The molecular organization of adrenal chromaffin granules.** *Neuroscience* 1980, *5* (11), 1803-1823.

[32] Falkensammer, G.; Fischer-Colbrie, R.; Winkler, H., **Biogenesis of Chromaffin Granules: Incorporation of Sulfate into Chromogranin B and into a Proteoglycan.** *Journal of Neurochemistry* 1985, *45* (5), 1475-1480.

[33] Helle, K. B.; Reed, R. K.; Pihl, K. E.; Serckhanssen, G., **Osmotic properties of the chromogranins and relation to osmotic-pressure in catecholamine storage granules.** *Acta Physiologica Scandinavica* 1985, *123* (1), 21-33.

[34] Borges, R.; Diaz-Vera, J.; Dominguez, N.; Arnau, M. R.; Machado, J. D., **Chromogranins as regulators of exocytosis.** *J. Neurochem.* 2010, *114* (2), 335-43.

[35] Liu, Y.; Edwards, R. H., **Differential Localization of Vesicular Acetylcholine and Monoamine Transporters in PC12 Cells but Not CHO Cells.** *The Journal of Cell Biology* 1997, *139* (4), 907-916.

[36] Varoqui, H.; Erickson, J. D., **Vesicular neurotransmitter transporters.** *Molecular Neurobiology* 1997, *15* (2), 165-191.

[37] Chaudhry, F. A.; Boulland, J. L.; Jenstad, M.; Bredahl, M. K.; Edwards, R. H., **Pharmacology of neurotransmitter transport into secretory vesicles.** *Handb. Exp. Pharmacol* 2008, (184), 77-106.

[38] Peter, D.; Jimenez, J.; Liu, Y.; Kim, J.; Edwards, R. H., **The chromaffin granule and synaptic vesicle amine transporters differ in substrate recognition and sensitivity to inhibitors.** *Journal of Biological Chemistry* 1994, *269* (10), 7231-7237.

[39] Peter, D.; Liu, Y.; Sternini, C.; de Giorgio, R.; Brecha, N.; Edwards, R. H., **Differential expression of two vesicular monoamine transporters.** *J. Neurosci.* 1995, *15* (9), 6179-88.

[40] Sulzer, D.; Bogulavsky, J.; Larsen, K. E.; Behr, G.; Karatekin, E.; Kleinman, M. H.; Turro, N.; Krantz, D.; Edwards, R. H.; Greene, L. A.; Zecca, L., **Neuromelanin biosynthesis is driven by excess cytosolic catecholamines not accumulated by synaptic vesicles.** *Proc. Natl. Acad. Sci. U S A* 2000, *97* (22), 11869-74.

[41] Hochman, J.; Perlman, R. L., **Catecholamine secretion by isolated adrenal cells.** *Biochim. Biophys. Acta* 1976, *421* (1), 168-75.

[42] Fenwick, E. M.; Fajdiga, P. B.; Howe, N. B.; Livett, B. G., **Functional and morphological characterization of isolated bovine adrenal medullary cells.** *J. Cell. Biol.* 1978, *76* (1), 12-30.

[43] Kobayashi, S.; Coupland, R. E., **Morphological aspects of chromaffin tissue: the differential fixation of adrenaline and noradrenaline.** *J. Anat.* 1993, *183 (Pt 2)*, 223-35.

[44] Verhofstad, A. A.; Coupland, R. E.; Parker, T. R.; Goldstein, M., **Immunohistochemical and biochemical study on the development of the noradrenaline- and adrenaline-storing cells of the adrenal medulla of the rat.** *Cell Tissue Res.* 1985, *242* (2), 233-43.

[45] Greene, L. A.; Tischler, A. S., **Establishment of a noradrenergic clonal line of rat adrenal pheochromocytoma cells which respond to nerve growth factor.** *Proc. Natl. Acad. Sci. U S A* 1976, *73* (7), 2424-8.

[46] Shafer, T. J.; Atchison, W. D., **Transmitter, ion channel and receptor properties of pheochromocytoma (PC12) cells: a model for neurotoxicological studies.** *Neurotoxicology* 1991, *12* (3), 473-92.

[47] Westerink, R. H. S.; Ewing, A. G., **The PC12 cell as model for neurosecretion.** *Acta physiologica (Oxford, England)* 2008, *192* (2), 273-285.

[48] Distler, A., **Role of Catecholamines in Blood Pressure Regulation. In *Hypertensive Cardiovascular Disease: Pathophysiology and Treatment,*** Amery, A.; Fagard, R.; Lijnen, P.; Staessen, J., Eds. Springer Netherlands: Dordrecht, 1982; pp 57-70.

[49] Carlsson, A.; Lindqvist, M.; Magnusson, T., **3,4-Dihydroxyphenylalanine and 5-hydroxytryptophan as reserpine antagonists.** *Nature* 1957, *180* (4596), 1200.

[50] Kobayashi, K., **Role of catecholamine signaling in brain and nervous system functions: new insights from mouse molecular genetic study.** *J. Investig. Dermatol. Symp Proc.* 2001, *6* (1), 115-21.

[51] Banerjee, D. K.; Lutz, R. A.; Levine, M. A.; Rodbard, D.; Pollard, H. B., **Uptake of norepinephrine and related catecholamines by cultured chromaffin cells: characterization of cocaine-sensitive and -insensitive plasma membrane transport sites.** *Proc. Natl. Acad. Sci. U S A* 1987, *84* (7), 1749-53.

[52] Eisenhofer, G.; Kopin, I. J.; Goldstein, D. S., **Catecholamine Metabolism: A Contemporary View with Implications for Physiology and Medicine.** *Pharmacological Reviews* 2004, *56* (3), 331-349.

[53] **Principles of pharmacology; the pathophysiologic basis of drug therapy.** Ringgold Inc: Portland, 2004; Vol. 28, p 122.

[54] Lyytinen, J.; Kaakkola, S.; Ahtila, S.; Tuomainen, P.; Teräväinen, H., **Simultaneous MAO-B and COMT inhibition in L-dopa-treated patients with parkinson's disease.** *Movement Disorders* 1997, *12* (4), 497-505.

[55] Birkmayer, W.; Hornykiewicz, O., **The L-3,4-dioxyphenylalanine (DOPA)-effect in Parkinson-akinesia.** *Wien Klin Wochenschr* 1961, *73*, 787-8.

[56] Mosharov, E. V.; Larsen, K. E.; Kanter, E.; Phillips, K. A.; Wilson, K.; Schmitz, Y.; Krantz, D. E.; Kobayashi, K.; Edwards, R. H.; Sulzer, D., **Interplay between Cytosolic Dopamine, Calcium, and α-Synuclein Causes Selective Death of Substantia Nigra Neurons.** *Neuron* 2009, *62* (2), 218-229.

[57] Pothos, E.; Desmond, M.; Sulzer, D., **L-3,4-dihydroxyphenylalanine increases the quantal size of exocytotic dopamine release in vitro.** *J. Neurochem.* 1996, *66* (2), 629-36.

[58] Mosharov, E. V.; Gong, L.-W.; Khanna, B.; Sulzer, D.; Lindau, M., **Intracellular Patch Electrochemistry: Regulation of Cytosolic Catecholamines in Chromaffin Cells.** *The Journal of Neuroscience* 2003, *23* (13), 5835-5845.

[59] Kittner, B.; Bräutigam, M.; Herken, H., **PC12 cells: a model system for studying drug effects on dopamine synthesis and release.** *Arch. Int. Pharmacodyn. Ther.* 1987, *286* (2), 181-194.

[60] Omiatek, D. M.; Dong, Y.; Heien, M. L.; Ewing, A. G., **Only a Fraction of Quantal Content is Released During Exocytosis as Revealed by Electrochemical Cytometry of Secretory Vesicles.** *ACS Chemical Neuroscience* 2010, *1* (3), 234-245.

[61] Li, X.; Majdi, S.; Dunevall, J.; Fathali, H.; Ewing, A. G., **Quantitative Measurement of Transmitters in Individual Vesicles in the Cytoplasm of Single Cells with Nanotip Electrodes.** *Angewandte Chemie International Edition* 2015, *54* (41), 11978-11982.

[62] Brodie, B. B.; Pletscher, A.; Shore, P. A., **Evidence that serotonin has a role in brain function.** *Science* 1955, *122* (3177), 968.

[63] Carlsson, A.; Hillarp, N. A., **Release of adenosine triphosphate along with adrenaline and noradrenaline following stimulation of the adrenal medulla.** *Acta Physiol. Scand.* 1956, *37* (2-3), 235-9.

[64] Schuldiner, S.; Shirvan, A.; Linial, M., **Vesicular neurotransmitter transporters: from bacteria to humans.** *Physiol. Rev.* 1995, *75* (2), 369-92.

[65] Darchen, F.; Scherman, D.; Henry, J. P., **Reserpine binding to chromaffin granules suggests the existence of two conformations of the monoamine transporter.** *Biochemistry* 1989, *28* (4), 1692-7.

[66] Schuldiner, S.; Liu, Y.; Edwards, R. H., **Reserpine binding to a vesicular amine transporter expressed in Chinese hamster ovary fibroblasts.** *J. Biol. Chem.* 1993, *268* (1), 29-34.

[67] Bangham, A. D.; Standish, M. M.; Watkins, J. C., **Diffusion of univalent ions across the lamellae of swollen phospholipids.** *J. Mol. Biol.* 1965, *13* (1), 238-52.

[68] Jesorka, A.; Orwar, O., **Liposomes: technologies and analytical applications.** *Annu. Rev. Anal. Chem. (Palo Alto Calif)* 2008, *1*, 801-32.

[69] Elizondo, E.; Moreno, E.; Cabrera, I.; Córdoba, A.; Sala, S.; Veciana, J.; Ventosa, N., **Liposomes and Other Vesicular Systems: Structural Characteristics, Methods of Preparation, and Use in Nanomedicine.** In *Progress in Molecular Biology and Translational Science*, Antonio, V., Ed. Academic Press: 2011; Vol. Volume 104, pp 1-52.

[70] Mozafari, M. R., **Nanoliposomes: preparation and analysis.** *Methods in molecular biology (Clifton, N.J.)* 2010, *605*, 29-50.

[71] Reineccius, G. A., **Liposomes for Controlled Release in the Food Industry. In *Encapsulation and Controlled Release of Food Ingredients,*** American Chemical Society: 1995; Vol. 590, pp 113-131.

[72] Lian, T.; Ho, R. J., **Trends and developments in liposome drug delivery systems.** *J. Pharm. Sci.* 2001, *90* (6), 667-80.

[73] Vemuri, S.; Rhodes, C. T., **Preparation and characterization of liposomes as therapeutic delivery systems: a review.** *Pharmaceutica Acta Helvetiae* 1995, *70* (2), 95-111.

[74] Gregoriadis, G., **Engineering liposomes for drug delivery: progress and problems.** *Trends in Biotechnology* 1995, *13* (12), 527-537.

[75] Chatterjee, S.; Banerjee, D. K., **Preparation, isolation, and characterization of liposomes containing natural and synthetic lipids.** *Methods in molecular biology (Clifton, N.J.)* 2002, *199*, 3-16.

[76] Pott, T.; Bouvrais, H.; Méléard, P., **Giant unilamellar vesicle formation under physiologically relevant conditions.** *Chemistry and Physics of Lipids* 2008, *154* (2), 115-119.

[77] Moscho, A.; Orwar, O.; Chiu, D. T.; Modi, B. P.; Zare, R. N., **Rapid preparation of giant unilamellar vesicles.** *Proceedings of the National Academy of Sciences* 1996, *93* (21), 11443-11447.

[78] Walter, H.; Brooks, D. E., **Phase separation in cytoplasm, due to macromolecular crowding, is the basis for microcompartmentation.** *FEBS Letters* 1995, *361* (2), 135-139.

[79] Pagliaro, L., **Mechanisms for cytoplasmic organization: An overview.** *Int. Rev. Cytol.* 2000, *192*, 303-318.

[80] Goobes, R.; Kahana, N.; Cohen, O.; Minsky, A., **Metabolic buffering exerted by macromolecular crowding on DNA-DNA interactions: origin and physiological significance.** *Biochemistry* 2003, *42* (8), 2431-40.

[81] Long, M. S.; Jones, C. D.; Helfrich, M. R.; Mangeney-Slavin, L. K.; Keating, C. D., **Dynamic microcompartmentation in synthetic cells.** *Proceedings of the National Academy of Sciences of the United States of America* 2005, *102* (17), 5920-5925.

[82] Albertsson, P. A., **Phase partition of cell particles and macromolecules.** *Trends in Biochemical Sciences* 1978, *3* (2), N37-N38.

[83] Helfrich, M. R.; Mangeney-Slavin, L. K.; Long, M. S.; Djoko, K. Y.; Keating, C. D., **Aqueous Phase Separation in Giant Vesicles.** *Journal of the American Chemical Society* 2002, *124* (45), 13374-13375.

[84] Keating, C. D., **Aqueous Phase Separation as a Possible Route to Compartmentalization of Biological Molecules.** *Accounts of Chemical Research* 2012, *45* (12), 2114-2124.

[85] Long, M. S.; Cans, A.-S.; Keating, C. D., **Budding and Asymmetric Protein Microcompartmentation in Giant Vesicles Containing Two Aqueous Phases.** *Journal of the American Chemical Society* 2008, *130* (2), 756-762.

[86] Tseng, Y.-L.; Liu, J.-J.; Hong, R.-L., **Translocation of Liposomes into Cancer Cells by Cell-Penetrating Peptides Penetratin and Tat: A Kinetic and Efficacy Study.** *Molecular Pharmacology* 2002, *62* (4), 864-872.

[87] Torchilin, V. P.; Rammohan, R.; Weissig, V.; Levchenko, T. S., **TAT peptide on the surface of liposomes affords their efficient intracellular delivery even at low temperature and in the presence of metabolic inhibitors.** *Proc. Natl. Acad. Sci. U S A* 2001, *98* (15), 8786-91.

[88] Nakase, I.; Niwa, M.; Takeuchi, T.; Sonomura, K.; Kawabata, N.; Koike, Y.; Takehashi, M.; Tanaka, S.; Ueda, K.; Simpson, J. C.; Jones, A. T.; Sugiura, Y.; Futaki, S., **Cellular uptake of arginine-rich peptides: roles for macropinocytosis and actin rearrangement.** *Mol. Ther.* 2004, *10* (6), 1011-22.

[89] Suzuki, T.; Futaki, S.; Niwa, M.; Tanaka, S.; Ueda, K.; Sugiura, Y., **Possible Existence of Common Internalization Mechanisms among Arginine-rich Peptides.** *Journal of Biological Chemistry* 2002, *277* (4), 2437-2443.

[90] Torchilin, V. P., **Recent advances with liposomes as pharmaceutical carriers.** *Nat. Rev. Drug. Discov.* 2005, *4* (2), 145-160.

[91] Futaki, S.; Ohashi, W.; Suzuki, T.; Niwa, M.; Tanaka, S.; Ueda, K.; Harashima, H.; Sugiura, Y., **Stearylated arginine-rich peptides: A new class of transfection systems.** *Bioconjugate Chemistry* 2001, *12* (6), 1005-1011.

[92] Iwasa, A.; Akita, H.; Khalil, I.; Kogure, K.; Futaki, S.; Harashima, H., **Cellular uptake and subsequent intracellular trafficking of R8-liposomes introduced at low temperature.** *Biochimica et Biophysica Acta (BBA) - Biomembranes* 2006, *1758* (6), 713-720.

[93] Rosenthal CK, e. a.; , **Milestones of Light Microscopy.** *Nature Milestones* 2009.

[94] Eugenio Fornasiero, S. O. R., **Super-Resolution Microscopy Techniques in the Neurosciences** 1st ed.; Humana Press, New York: 2014.

[95] König, K., **Handbook of Biological Confocal Microscopy.** Third Edition ed.; Springer Science+Business Media: New York, 2006.

[96] Bozzola, J. J., **Electron Microscopy.** In *eLS*, John Wiley & Sons, Ltd: 2001.

[97] Williams, D. B.; Carter, C. B., **The Transmission Electron Microscope. In Transmission Electron Microscopy: A Textbook for Materials Science,** Springer US: Boston, MA, 1996; pp 3-17.

[98] Thornton, P. R., **Scanning electron microscopy: applications to materials and device science.** London, 1968.

[99] Palade, G. E., **A study of fixation for electron microscopy.** *J. Exp. Med.* 1952, *95* (3), 285-98.

[100] Sabatini, D. D.; Bensch, K.; Barrnett, R. J., **Cytochemistry and electron microscopy. The preservation of cellular ultrastructure and enzymatic activity by aldehyde fixation.** *J. Cell Biol.* 1963, *17*, 19-58.

[101] Morris, J. K., **A formaldehyde glutaraldehyde fixative of high osmolality for use in electron microscopy.** *J. Cell Biol* 1965, *27*, 137.

[102] Harris, J. R., **Principles and techniques of electron microscopy biological applications**: M. A. Hayat, Fourth Edition (2000), Cambridge University Press, Cambridge, UK. Hardback, 543 pp, *Micron* 2002, *33* (3), 325-326.

[103] Hawes, P.; Netherton, C. L.; Mueller, M.; Wileman, T.; Monaghan, P., **Rapid freeze-substitution preserves membranes in high-pressure frozen tissue culture cells.** *J. Microsc.* 2007, *226* (Pt 2), 182-9.

[104] Hurbain, I.; Sachse, M., **The future is cold: cryo-preparation methods for transmission electron microscopy of cells.** *Biol. Cell* 2011, *103* (9), 405-20.

[105] Walther, P.; Ziegler, A., **Freeze substitution of high-pressure frozen samples: the visibility of biological membranes is improved when the substitution medium contains water.** *J. Microsc.* 2002, *208* (Pt 1), 3-10.

[106] Goldstein, J. I., **Scanning electron microscopy and x-ray microanalysis: a text for biologists, materials scientists and geologists.** Plenum: New York, 1992; Vol. 2.

[107] Heckman, C.; Kanagasundaram, S.; Cayer, M.; Paige, J., **Preparation of cultured cells for scanning electron microscope.** 2007.

[108] Karas, M.; Bachmann, D.; Hillenkamp, F., **Influence of the wavelength in high-irradiance ultraviolet laser desorption mass spectrometry of organic molecules.** *Analytical Chemistry* 1985, *57* (14), 2935-2939.

[109] Gessel, M. M.; Norris, J. L.; Caprioli, R. M., **MALDI Imaging Mass Spectrometry: Spatial Molecular Analysis to Enable a New Age of Discovery.** *Journal of proteomics* 2014, *0*, 71-82.

[110] Chughtai, K.; Heeren, R. M. A., **Mass Spectrometric Imaging for Biomedical Tissue Analysis.** *Chemical Reviews* 2010, *110* (5), 3237-3277.

[111] Thiery-Lavenant, G.; Zavalin, A. I.; Caprioli, R. M., **Targeted multiplex imaging mass spectrometry in transmission geometry for subcellular spatial resolution.** *J. Am. Soc. Mass Spectrom.* 2013, *24* (4), 609-14.

[112] Boxer, S. G.; Kraft, M. L.; Weber, P. K., **Advances in Imaging Secondary Ion Mass Spectrometry for Biological Samples.** *Annual Review of Biophysics* 2009, *38* (1), 53-74.

[113] Fletcher, J. S.; Vickerman, J. C., **Secondary Ion Mass Spectrometry: Characterizing Complex Samples in Two and Three Dimensions.** *Analytical Chemistry* 2013, *85* (2), 610-639.

[114] Vickerman, J. C., **Molecular Surface Mass Spectrometry by SIMS.** In *Surface Analysis – The Principal Techniques*, John Wiley & Sons, Ltd: 2009; pp 113-205.

[115] Zimmerman, T. A.; Monroe, E. B.; Tucker, K. R.; Rubakhin, S. S.; Sweedler, J. V., Chapter 13: **Imaging of cells and tissues with mass spectrometry: adding chemical information to imaging.** *Methods in cell biology* 2008, *89*, 361-90.

[116] Fletcher, J. S.; Lockyer, N. P.; Vickerman, J. C., **Developments in molecular SIMS depth profiling and 3D imaging of biological systems using polyatomic primary ions.** *Mass Spectrometry Reviews* 2011, *30* (1), 142-174.

[117] Belu, A. M.; Graham, D. J.; Castner, D. G., **Time-of-flight secondary ion mass spectrometry: techniques and applications for the characterization of biomaterial surfaces.** *Biomaterials* 2003, *24* (21), 3635-3653.

[118] Hoppe, P.; Cohen, S.; Meibom, A., **NanoSIMS: Technical Aspects and Applications in Cosmochemistry and Biological Geochemistry.** *Geostandards and Geoanalytical Research* 2013, *37* (2), 111-154.

[119] Kilburn, M. R.; Wacey, D., **CHAPTER 1 Nanoscale Secondary Ion Mass Spectrometry (NanoSIMS) as an Analytical Tool in the Geosciences. In *Principles and Practice of Analytical Techniques in Geosciences,*** The Royal Society of Chemistry: 2015; pp 1-34.

[120] Kilburn, M. R.; Clode, P. L., **Elemental and isotopic imaging of biological samples using NanoSIMS.** *Methods in molecular biology (Clifton, N.J.)* 2014, *1117*, 733-55.

[121] Benninghoven, A.; Jaspers, D.; Sichtermann, W., **Secondary-ion emission of amino acids.** *Applied physics* 1976, *11* (1), 35-39.

[122] Vickerman, J.; Winograd, N., **Cluster TOF-SIMS Imaging and the Characterization of Biological Materials.** In *Cluster Secondary Ion Mass Spectrometry*, John Wiley & Sons, Inc.: 2013; pp 269-312.

[123] Guerquin-Kern, J.-L.; Wu, T.-D.; Quintana, C.; Croisy, A., **Progress in analytical imaging of the cell by dynamic secondary ion mass spectrometry (SIMS microscopy).** *Biochimica et Biophysica Acta (BBA) - General Subjects* 2005, *1724* (3), 228-238.

[124] Chandra, S.; Smith, D. R.; Morrison, G. H., **Subcellular imaging by dynamic SIMS ion microscopy.** *Anal. Chem.* 2000, *72* (3), 104A-114A.

[125] RAGHAVAN, V., **Materials science and engineering: a first course.** PHI Learning: 2004.

[126] Kollmer, F., **Cluster primary ion bombardment of organic materials.** *Applied Surface Science* 2004, *231–232*, 153-158.

[127] Nygren, H.; Malmberg, P., **High resolution imaging by organic secondary ion mass spectrometry.** *Trends in Biotechnology* 2007, *25* (11), 499-504.

[128] Malherbe, J.; Penen, F.; Isaure, M.-P.; Frank, J.; Hause, G.; Dobritzsch, D.; Gontier, E.; Horréard, F.; Hillion, F.; Schaumlöffel, D., **A New Radio Frequency Plasma Oxygen Primary Ion Source on Nano Secondary Ion Mass Spectrometry for Improved Lateral Resolution and Detection of Electropositive Elements at Single Cell Level.** *Analytical Chemistry* 2016, *88* (14), 7130-7136.

[129] Vickerman, J. C.; Winograd, N., SIMS—**A precursor and partner to contemporary mass spectrometry.** *International Journal of Mass Spectrometry* 2015, *377*, 568-579.

[130] Wittmaack, K., **Secondary-ion emission from silicon bombarded with atomic and molecular noble-gas ions.** *Surface Science* 1979, *90* (2), 557-563.

[131] Kollmer, F., **Cluster primary ion bombardment of organic materials.** *Applied Surface Science* 2004, *231–232* (0), 153-158.

[132] Weibel, D.; Wong, S.; Lockyer, N.; Blenkinsopp, P.; Hill, R.; Vickerman, J. C., **A C60 primary ion beam system for time of flight secondary ion mass spectrometry: Its development and secondary ion yield characteristics.** *Analytical Chemistry* 2003, *75* (7), 1754-1764.

[133] Fletcher, J. S.; Rabbani, S.; Barber, A. M.; Lockyer, N. P.; Vickerman, J. C., **Comparison of C60 and GCIB primary ion beams for the analysis of cancer cells and tumour sections.** *Surface and Interface Analysis* 2013, *45* (1), 273-276.

[134] Paul, W., **Electromagnetic Traps for Charged and Neutral Particles (Nobel Lecture).** *Angewandte Chemie International Edition in English* 1990, *29* (7), 739-748.

[135] Benninghoven, A., **Chemical Analysis of Inorganic and Organic Surfaces and Thin Films by Static Time-of-Flight Secondary Ion Mass Spectrometry (TOF-SIMS).** *Angewandte Chemie International Edition in English* 1994, *33* (10), 1023-1043.

[136] R. Castaing, G. S., **Microanalyse par e´mission ionique secondaire.** *J. Microsc.* 1962, *1*, 395–410.

[137] Briggs, D.; Fletcher, I. W.; Reichlmaier, S.; AguloSanchez, J. L.; Short, R. D., **SIMS applied to polymer surfaces. 18. Surface morphology of a PVC/PMMA blend studied by ToF-SIMS.** *Surface and Interface Analysis* 1996, *24* (6), 419-421.

[138] Nygren, H.; Eriksson, C.; Hederstierna, K.; Malmberg, P., **TOF-SIMS analysis of the interface between bone and titanium implants—Effect of porosity and magnesium coating.** *Applied Surface Science* 2008, *255* (4), 1092-1095.

[139] Brunelle, A.; Touboul, D.; Laprevote, O., **Biological tissue imaging with time-of-flight secondary ion mass spectrometry and cluster ion sources.** *J. Mass Spectrom.* 2005, *40* (8), 985-999.

[140] Fletcher, J. S., **Cellular imaging with secondary ion mass spectrometry.** *Analyst* 2009, *134* (11), 2204-2215.

[141] Fletcher, J. S.; Vickerman, J. C.; Winograd, N., **Label free biochemical 2D and 3D imaging using secondary ion mass spectrometry.** *Current Opinion in Chemical Biology* 2011, *15* (5), 733-740.

[142] Ostrowski, S. G.; Van Bell, C. T.; Winograd, N.; Ewing, A. G., **Mass spectrometric imaging of highly curved membranes during Tetrahymena mating.** *Science* 2004, *305* (5680), 71-3.

[143] Kurczy, M. E.; Piehowski, P. D.; Van Bell, C. T.; Heien, M. L.; Winograd, N.; Ewing, A. G., **Mass spectrometry imaging of mating Tetrahymena show that changes in cell morphology regulate lipid domain formation.** *Proceedings of the National Academy of Sciences* 2010, *107* (7), 2751-2756.

[144] Pacholski, M. L.; Cannon, D. M.; Ewing, A. G.; Winograd, N., **Static time-of-flight secondary ion mass spectrometry imaging of freeze-fractured, frozen-hydrated biological membranes.** *Rapid Commun. Mass Spectrom.* 1998, *12* (18), 1232-1235.

[145] Sodhi, R. N. S., **Time-of-flight secondary ion mass spectrometry (TOF-SIMS): versatility in chemical and imaging surface analysis.** *Analyst* 2004, *129* (6), 483-487.

[146] Nygren, H.; Hagenhoff, B.; Malmberg, P.; Nilsson, M.; Richter, K., **Bioimaging TOF-SIMS: High resolution 3D imaging of single cells.** *Microscopy Research and Technique* 2007, *70* (11), 969-974.

[147] Debois, D.; Brunelle, A.; Laprévote, O., **Attempts for molecular depth profiling directly on a rat brain tissue section using fullerene and bismuth cluster ion beams.** *International Journal of Mass Spectrometry* 2007, *260* (2–3), 115-120.

[148] Gilmore, I. S.; Seah, M. P., **Electron flood gun damage in the analysis of polymers and organics in time-of-flight SIMS.** *Applied Surface Science* 2002, *187* (1–2), 89-100.

[149] Havelund, R.; Seah, M. P.; Shard, A. G.; Gilmore, I. S., **Electron Flood Gun Damage Effects in 3D Secondary Ion Mass Spectrometry Imaging of Organics.** *Journal of The American Society for Mass Spectrometry* 2014, *25* (9), 1565-1571.

[150] Lee, J. L. S.; Gilmore, I. S.; Seah, M. P.; Fletcher, I. W., **Topography and Field Effects in Secondary Ion Mass Spectrometry – Part I: Conducting Samples.** *Journal of The American Society for Mass Spectrometry* 2011, *22* (10), 1718-1728.

[151] Hagenhoff, B., **High Resolution Surface Analysis by TOF-SIMS.** *Microchimica Acta* 2000, *132* (2), 259-271.

[152] Jones, E. A.; Lockyer, N. P.; Vickerman, J. C., **Mass spectral analysis and imaging of tissue by ToF-SIMS—The role of buckminsterfullerene, C_{60}^+, primary ions.** *International Journal of Mass Spectrometry* 2007, *260* (2–3), 146-157.

[153] Kurczy, M. E.; Piehowski, P. D.; Parry, S. A.; Jiang, M.; Chen, G.; Ewing, A. G.; Winograd, N., **Which is more important in bioimaging SIMS experiments—The sample preparation or the nature of the projectile?** *Applied Surface Science* 2008, *255* (4), 1298-1304.

[154] Cannon, D. M.; Pacholski, M. L.; Winograd, N.; Ewing, A. G., **Molecule Specific Imaging of Freeze-Fractured, Frozen-Hydrated Model Membrane Systems Using Mass Spectrometry.** *Journal of the American Chemical Society* 2000, *122* (4), 603-610.

[155] Kurczy, M. E.; Piehowski, P. D.; Willingham, D.; Molyneaux, K. A.; Heien, M. L.; Winograd, N.; Ewing, A. G., **Nanotome Cluster Bombardment to Recover Spatial Chemistry after Preparation of Biological Samples for SIMS Imaging.** *Journal of the American Society for Mass Spectrometry* 2010, *21* (5), 833-836.

[156] Brunelle, A.; Laprevote, O., **Recent advances in biological tissue imaging with Time-of-flight Secondary Ion Mass Spectrometry: polyatomic ion sources, sample preparation, and applications.** *Curr. Pharm. Des.* 2007, *13* (32), 3335-43.

[157] Lanekoff, I.; Kurczy, M. E.; Hill, R.; Fletcher, J. S.; Vickerman, J. C.; Winograd, N.; Sjövall, P.; Ewing, A. G., **Time of Flight Mass Spectrometry Imaging of Samples Fractured In Situ with a Spring-Loaded Trap System.** *Analytical Chemistry* 2010, *82* (15), 6652-6659.

[158] Lozano-Perez, S.; Schröder, M.; Yamada, T.; Terachi, T.; English, C. A.; Grovenor, C. R. M., Using **NanoSIMS to map trace elements in stainless steels from nuclear reactors.** *Applied Surface Science* 2008, *255* (4), 1541-1543.

[159] Moore, K. L.; Lombi, E.; Zhao, F.-J.; Grovenor, C. R. M., **Elemental imaging at the nanoscale: NanoSIMS and complementary techniques for element localisation in plants.** *Analytical and Bioanalytical Chemistry* 2011, *402* (10), 3263-3273.

[160] Inagaki, F.; Hinrichs, K.-U.; Kubo, Y.; Bowles, M. W.; Heuer, V. B.; Hong, W.-L.; Hoshino, T.; Ijiri, A.; Imachi, H.; Ito, M.; Kaneko, M.; Lever, M. A.; Lin, Y.-S.; Methé, B. A.; Morita, S.; Morono, Y.; Tanikawa, W.; Bihan, M.; Bowden, S. A.; Elvert, M.; Glombitza, C.; Gross, D.; Harrington, G. J.; Hori, T.; Li, K.; Limmer, D.; Liu, C.-H.; Murayama, M.; Ohkouchi, N.; Ono, S.; Park, Y.-S.; Phillips, S. C.; Prieto-Mollar, X.; Purkey, M.; Riedinger, N.; Sanada, Y.; Sauvage, J.; Snyder, G.; Susilawati, R.; Takano, Y.; Tasumi, E.; Terada, T.; Tomaru, H.; Trembath-Reichert, E.; Wang, D. T.; Yamada, Y., **Exploring deep microbial life in coal-bearing sediment down to ~2.5 km below the ocean floor.** *Science* 2015, *349* (6246), 420-424.

[161] Steinhauser, M. L.; Bailey, A. P.; Senyo, S. E.; Guillermier, C.; Perlstein, T. S.; Gould, A. P.; Lee, R. T.; Lechene, C. P., **Multi-isotope imaging mass spectrometry quantifies stem cell division and metabolism.** *Nature* 2012, *481* (7382), 516-519.

[162] Brismar, H.; Aperia, A.; Westin, L.; Moy, J.; Wang, M.; Guillermier, C.; Poczatek, C.; Lechene, C., **Study of protein and RNA in dendritic spines using multi-isotope imaging mass spectrometry (MIMS).** *Surface and interface analysis : SIA* 2014, *46* (Suppl 1), 158-160.

[163] McMahon, G.; Glassner, B. J.; Lechene, C. P., **Quantitative imaging of cells with multi-isotope imaging mass spectrometry (MIMS)—Nanoautography with stable isotope tracers.** *Applied Surface Science* 2006, *252* (19), 6895-6906.

[164] Grovenor, C. R. M.; Smart, K. E.; Kilburn, M. R.; Shore, B.; Dilworth, J. R.; Martin, B.; Hawes, C.; Rickaby, R. E. M., **Specimen preparation for NanoSIMS analysis of biological materials.** *Applied Surface Science* 2006, *252* (19), 6917-6924.

[165] Galli Marxer, C.; Kraft, M. L.; Weber, P. K.; Hutcheon, I. D.; Boxer, S. G., **Supported Membrane Composition Analysis by Secondary Ion Mass Spectrometry with High Lateral Resolution.** *Biophysical Journal* 2005, *88* (4), 2965-2975.

[166] Lozano, M. M.; Liu, Z.; Sunnick, E.; Janshoff, A.; Kumar, K.; Boxer, S. G., **Colocalization of the ganglioside G(M1) and cholesterol detected by secondary ion mass spectrometry.** *J. Am. Chem. Soc.* 2013, *135* (15), 5620-30.

[167] Takado, Y.; Knott, G.; Humbel, B. M.; Escrig, S.; Masoodi, M.; Meibom, A.; Comment, A., **Imaging liver and brain glycogen metabolism at the nanometer scale.** *Nanomedicine: Nanotechnology, Biology and Medicine* 2015, *11* (1), 239-245.

[168] Saka, S. K.; Vogts, A.; Krohnert, K.; Hillion, F.; Rizzoli, S. O.; Wessels, J. T., **Correlated optical and isotopic nanoscopy.** *Nat. Commun.* 2014, *5*, 8.

[169] Angelo, M.; Bendall, S. C.; Finck, R.; Hale, M. B.; Hitzman, C.; Borowsky, A. D.; Levenson, R. M.; Lowe, J. B.; Liu, S. D.; Zhao, S.; Natkunam, Y.; Nolan, G. P., **Multiplexed ion beam imaging of human breast tumors.** *Nat. Med.* 2014, *20* (4), 436-442.

[170] Opazo, F.; Levy, M.; Byrom, M.; Schafer, C.; Geisler, C.; Groemer, T. W.; Ellington, A. D.; Rizzoli, S. O., **Aptamers as potential tools for super-resolution microscopy.** *Nat. Meth.* 2012, *9* (10), 938-939.

[171] Vreja, I. C.; Kabatas, S.; Saka, S. K.; Krohnert, K.; Hoschen, C.; Opazo, F.; Diederichsen, U.; Rizzoli, S. O., **Secondary-Ion Mass Spectrometry of Genetically Encoded Targets.** *Angew. Chem.-Int. Edit.* 2015, *54* (19), 5784-5788.

[172] Adams, R. N., **Probing brain chemistry with electroanalytical techniques.** *Analytical Chemistry* 1976, *48* (14), 1126A-1138A.

[173] Wightman, R. M.; Jankowski, J. A.; Kennedy, R. T.; Kawagoe, K. T.; Schroeder, T. J.; Leszczyszyn, D. J.; Near, J. A.; Diliberto, E. J.; Viveros, O. H., **Temporally resolved catecholamine spikes correspond to single vesicle release from individual chromaffin cells.** *Proceedings of the National Academy of Sciences of the United States of America* 1991, *88* (23), 10754-10758.

[174] Leszczyszyn, D. J.; Jankowski, J. A.; Viveros, O. H.; Diliberto, E. J., Jr.; Near, J. A.; Wightman, R. M., **Secretion of catecholamines from individual adrenal medullary chromaffin cells.** *J. Neurochem.* 1991, *56* (6), 1855-63.

[175] Travis, E. R.; Wightman, R. M., **Spatio-temporal resolution of exocytosis from individual cells.** *Annu. Rev. Biophys. Biomol. Struct.* 1998, *27*, 77-103.

[176] Heien, M. L.; Johnson, M. A.; Wightman, R. M., **Resolving neurotransmitters detected by fast-scan cyclic voltammetry.** *Anal. Chem.* 2004, *76* (19), 5697-704.

[177] Kozminski, K. D.; Gutman, D. A.; Davila, V.; Sulzer, D.; Ewing, A. G., **Voltammetric and pharmacological characterization of dopamine release from single exocytotic events at rat pheochromocytoma (PC12) cells.** *Anal. Chem.* 1998, *70* (15), 3123-30.

[178] Michael, A. C.; Borland, L. M.; Free, N. B.-. **Electrochemical methods for neuroscience.** CRC Press/Taylor & Francis: Boca Raton, 2007; Vol. 33.

[179] Kim, D.; Koseoglu, S.; Manning, B. M.; Meyer, A. F.; Haynes, C. L., **Electroanalytical Eavesdropping on Single Cell Communication.** *Analytical chemistry* 2011, *83* (19), 7242-7249.

[180] Ponchon, J. L.; Cespuglio, R.; Gonon, F.; Jouvet, M.; Pujol, J. F., **Normal pulse polarography with carbon fiber electrodes for in vitro and in vivo determination of catecholamines.** *Analytical Chemistry* 1979, *51* (9), 1483-1486.

[181] Dayton, M. A.; Brown, J. C.; Stutts, K. J.; Wightman, R. M., **Faradaic electrochemistry at microvoltammetric electrodes.** *Analytical Chemistry* 1980, *52* (6), 946-950.

[182] Leszczyszyn, D. J.; Jankowski, J. A.; Viveros, O. H.; Diliberto, E. J., Jr.; Near, J. A.; Wightman, R. M., **Nicotinic receptor-mediated catecholamine secretion from individual chromaffin cells. Chemical evidence for exocytosis.** *J. Biol. Chem.* 1990, *265* (25), 14736-7.

[183] Finnegan, J. M.; Pihel, K.; Cahill, P. S.; Huang, L.; Zerby, S. E.; Ewing, A. G.; Kennedy, R. T.; Wightman, R. M., **Vesicular quantal size measured by amperometry at chromaffin, mast, pheochromocytoma, and pancreatic beta-cells.** *J. Neurochem.* 1996, *66* (5), 1914-23.

[184] Chen, T. K.; Luo, G.; Ewing, A. G., **Amperometric Monitoring of Stimulated Catecholamine Release from Rat Pheochromocytoma (PC12) Cells at the Zeptomole Level.** *Analytical Chemistry* 1994, *66* (19), 3031-3035.

[185] Koh, D.-S.; Hille, B., **Modulation by neurotransmitters of catecholamine secretion from sympathetic ganglion neurons detected by amperometry.** *Proceedings of the National Academy of Sciences* 1997, *94* (4), 1506-1511.

[186] Hochstetler, S. E.; Puopolo, M.; Gustincich, S.; Raviola, E.; Wightman, R. M., **Real-time amperometric measurements of zeptomole quantities of dopamine released from neurons.** *Anal. Chem.* 2000, *72* (3), 489-96.

[187] Cans, A.-S.; Ewing, A. G., **Highlights of 20 years of electrochemical measurements of exocytosis at cells and artificial cells.** *Journal of Solid State Electrochemistry* 2011, *15* (7), 1437-1450.

[188] Mellander, L.; Cans, A.-S.; Ewing, A. G., **Electrochemical Probes for Detection and Analysis of Exocytosis and Vesicles.** *ChemPhysChem* 2010, *11* (13), 2756-2763.

[189] Mosharov, E. V.; Sulzer, D., **Analysis of exocytotic events recorded by amperometry.** *Nat. Meth.* 2005, *2* (9), 651-658.

[190] Omiatek, D. M.; Santillo, M. F.; Heien, M. L.; Ewing, A. G., **Hybrid Capillary-Microfluidic Device for the Separation, Lysis, and Electrochemical Detection of Vesicles.** *Analytical Chemistry* 2009, *81* (6), 2294-2302.

[191] Omiatek, D. M.; Bressler, A. J.; Cans, A.-S.; Andrews, A. M.; Heien, M. L.; Ewing, A. G., **The real catecholamine content of secretory vesicles in the CNS revealed by electrochemical cytometry.** *Scientific Reports* 2013, *3*, 1447.

[192] Kim, B.-K.; Boika, A.; Kim, J.; Dick, J. E.; Bard, A. J., **Characterizing Emulsions by Observation of Single Droplet Collisions—Attoliter Electrochemical Reactors.** *Journal of the American Chemical Society* 2014, *136* (13), 4849-4852.

[193] Cheng, W.; Compton, R. G., **Investigation of Single-Drug-Encapsulating Liposomes using the Nano-Impact Method.** *Angewandte Chemie International Edition* 2014, *53* (50), 13928-13930.

[194] Dunevall, J.; Fathali, H.; Najafinobar, N.; Lovric, J.; Wigström, J.; Cans, A.-S.; Ewing, A. G., **Characterizing the Catecholamine Content of Single Mammalian Vesicles by Collision–Adsorption Events at an Electrode.** *Journal of the American Chemical Society* 2015, *137* (13), 4344-4346.

[195] Lovric, J.; Najafinobar, N.; Dunevall, J.; Majdi, S.; Svir, I.; Oleinick, A.; Amatore, C.; Ewing, A., **On the mechanism of electrochemical vesicle cytometry: chromaffin cell vesicles and liposomes.** *Faraday Discussions* 2016.

[196] Strein, T. G.; Ewing, A. G., **Characterization of submicron-sized carbon electrodes insulated with a phenol-allylphenol copolymer.** *Analytical Chemistry* 1992, *64* (13), 1368-1373.

9 APPENDIX (PAPERS I-V)